Molecular Pharmacology Fast Forward. Published on July 21, 2021 as DOI: 10.1124/molpharm.121.000280
This article has not been copyedited and formatted. The final version may differ from this version.

Title: Dynamic Expression of TRPV3 and Integrated Signaling with Growth Factor Pathways During Lung Epithelial Wound Repair Following Wood Smoke Particle and Other Forms of Lung Cell Injury

Authors: Katherine L. Burrell, Nam D. Nguyen, Cassandra E. Deering-Rice, Tosifa A. Memon, Marysol Almestica-Roberts, Emmanuel Rapp, Samantha N. Serna, John G. Lamb, and Christopher A. Reilly

Affiliations: (KLB, NDN, CEDR, TAM, MAR, ER, SNS, JGL, CAR) Department of Pharmacology and Toxicology, Center for Human Toxicology, University of Utah, 30 S 2000 E, Room 201 Skaggs Hall, Salt Lake City, Utah 84112, United States

Downloaded from molpharm.aspetjournals.org at ASPET Journals on March 20, 2024

Molecular Pharmacology Fast Forward. Published on July 21, 2021 as DOI: 10.1124/molpharm.121.000280
This article has not been copyedited and formatted. The final version may differ from this version.

Running Title: Dynamic Regulation of TRPV3 in Injured Lung Cells

Corresponding Author:
Christopher A. Reilly, Ph.D.
Department of Pharmacology and Toxicology, Center for Human Toxicology
University of Utah
30 S. 2000 E., Room 201 Skaggs Hall
Salt Lake City, UT 84112,
Phone: 801-581-5236
Email: Chris.Reilly@pharm.utah.edu

Number of text pages: 38
Number of Tables: 1
Number of Figures: 10
References: 48
Number of words in Abstract: 241
Number of words in Introduction: 741
Number of words in Discussion: 1412

Non-Standard Abbreviations: TRPV3, transient receptor potential vanilloid-3; WSPM, wood smoke particulate matter; HBEC, human bronchial epithelial cell; TRPA1, transient receptor potential ankyrin-1; EGFR/ErbB1, epidermal growth factor receptor; Wnt (7a), wingless-type MMTV integration site family (member 7a); TGFβ1 and β2, transforming growth factors beta 1 and beta 2; ERS, endoplasmic reticulum stress; DDIT3, DNA damage inducible transcript-3; eIF2αK3, protein kinase R-like endoplasmic reticulum kinase; DEP, diesel exhaust particulate; MUC5AC and 5B, oligomeric gel-forming mucins 5AA and 5B. MUC4, cell surface associated mucin, 4; ATP, adenosine triphosphate; H_2O_2, hydrogen peroxide; Ca^{2+}, calcium ion; TRPC1, transient receptor potential canonical-1; TRPV2, transient receptor potential vanilloid-2; TRPV4, transient receptor potential vanilloid-4; TRPM7, transient receptor potential melastatin-7; TRPM8, transient receptor potential melastatin-8; ErbB2, HER2/receptor tyrosine kinase 2; ErbB4, HER4/receptor tyrosine kinase 4; TGFβRI and RII, transforming growth factor receptors beta 1 and beta 2; HB-EGF, heparin-binding EGF like growth factor; EPGN, epithelial mitogen; NRG1, neuregulin 1; AREG, amphiregulin; EREG, epiregulin; sFRP-1, secreted frizzled related protein 1; p38 MAPK, mitogen-activated protein kinase 14; GSK3β, glycogen synthase kinase 3 beta; JNK, mitogen-activated protein kinase 8; NF-kB, nuclear factor kappa B; FZD5, frizzled class receptor 5; HBEC-3KT, normal human bronchial epithelial cells immortalized with CDK4 and hTERT; BEAS-2B, human bronchial epithelial cells; B2BV3OE, BEAS-2B cells stably overexpressing TRPV3; TRPV3KO, HBEC3-KT where TRPV3 has been knocked out; LHC-9, Lechner and LaVeck media; PBS, phosphate-buffered saline; PCR, polymerase chain reaction; qPCR, quantitative real-time PCR; β2M, beta-2 microglobulin; OPA, oropharyngeal aspiration; i.p., intra-peritoneal; ANOVA, analysis of variance; EMT, epithelial to mesenchymal, TGFα, transforming growth factor alpha; SMAD, TGF family receptor.

Keywords: Lung epithelium, wound repair, TRP channels, EGFR, growth factors

Downloaded from molpharm.aspetjournals.org at ASPET Journals on March 20, 2024

Molecular Pharmacology Fast Forward. Published on July 21, 2021 as DOI: 10.1124/molpharm.121.000280
This article has not been copyedited and formatted. The final version may differ from this version.

Abstract:

Prior studies revealed increased expression of the transient receptor potential vanilloid-3 (TRPV3) ion channel following wood smoke particulate matter (WSPM) treatment of human bronchial epithelial cells (HBECs). TRPV3 attenuated pathological endoplasmic reticulum stress and cytotoxicity mediated by TRP ankyrin-1 (TRPA1). Here, the basis for how TRPV3 expression is regulated by cell injury, the effects this has on HBEC physiology and WSPM-induced airway remodeling in mice was investigated. TRPV3 mRNA was rapidly increased in HBECs treated with WSPM and after monolayer damage caused by tryptic disruption, scratch wounding, and cell passaging. TRPV3 mRNA abundance varied with time, and stimulated expression occurred independent of new protein synthesis. Over-expression of TRPV3 in HBECs reduced cell migration and wound repair, while enhancing cell adhesion. This phenotype correlated with disrupted mRNA expression of ligands of the epidermal growth factor, tumor growth factor-β, and frizzled receptors. Accordingly, delayed wound repair by TRPV3 overexpressing cells was reversed by growth factor supplementation. In normal HBECs, TRPV3 up-regulation was triggered by exogenous growth factor supplementation, and was attenuated by inhibitors of growth factor receptor signaling. In mice, sub-acute oropharyngeal instillation with WSPM also promoted TRPV3 mRNA expression and epithelial remodeling, which was attenuated by TRPV3 antagonist pre- and co-treatment. This latter effect may be the consequence of antagonist-induced TRPV3 expression. These findings provide insights into the roles of TRPV3 in lung epithelial cells under basal and dynamic states, as well as highlight potential roles for TRPV3 ligands in modulating epithelial damage/repair.

Downloaded from molpharm.aspetjournals.org at ASPET Journals on March 20, 2024

Molecular Pharmacology Fast Forward. Published on July 21, 2021 as DOI: 10.1124/molpharm.121.000280
This article has not been copyedited and formatted. The final version may differ from this version.

Significance Statement:

Coordinated epithelial repair is essential for the maintenance of the airways, with deficiencies and over- repair associated with adverse consequences to respiratory health. This study shows that TRPV3, an ion channel, is involved in coordinating repair through integrated repair signaling pathways, wherein TRPV3 expression is up-regulated immediately following injury, and returns to basal levels as cells complete the repair process. TRPV3 may be a novel target for understanding and/or treating conditions in which airway/lung epithelial repair is not properly orchestrated.

Downloaded from molpharm.aspetjournals.org at ASPET Journals on March 20, 2024

Molecular Pharmacology Fast Forward. Published on July 21, 2021 as DOI: 10.1124/molpharm.121.000280
This article has not been copyedited and formatted. The final version may differ from this version.

Introduction:

Particulate matter (PM) derived from burning wood and biomass (WSPM) is a specific and pervasive type of air pollutant. WSPM exposure is associated with increased rates of hospital admissions for respiratory complications (Swiston *et al.*, 2008; Ghio *et al.*, 2012; Reid *et al.*, 2016; Liu *et al.*, 2017), while long-term exposure causes and exacerbates chronic diseases including asthma and chronic obstructive pulmonary disorder (Laumbach and Kipen, 2012; Olloquequi and Silva O, 2016).

How WSPM affects the respiratory tract is not fully understood. Our laboratory demonstrated that pine, mesquite, and other biomass smoke PM activate the transient receptor potential ankyrin-1 (TRPA1) and vanilloid-3 (TRPV3) ion channels (Shapiro *et al.*, 2013; Deering-Rice *et al.*, 2018). Activation of TRPA1 by WSPM in human bronchial epithelial cells (HBECs) causes endoplasmic reticulum Ca^{2+} depletion and activation of the eukaryotic translation initiation factor 2-alpha kinase-3 (eIF2αK3)-dependent branch of the endoplasmic reticulum stress (ERS) response. This pathway promotes pro-apoptotic DNA damage-inducible transcript-3 (DDIT3) expression and cell death. Additionally, pine and other forms of WSPM, pure TRPA1 agonists, and diesel exhaust particles (DEP), stimulate the expression and secretion of gel-forming mucins (MUC5AC and 5B), and the EGFR ligand MUC4 in HBECs (Deering-Rice *et al.*, 2019; Memon *et al.*, 2020).

The consequences of TRPV3 activation in HBECs by WSPM and other substances are not fully understood. The discovery that TRPV3 expression increases in HBECs following treatment with cytotoxic concentrations of WSPM and TRPA1 agonists, and that TRPV3 counteracts TRPA1 activity, ERS, and cytotoxicity, provides clues that TRPV3 may be critical for adaptation of lung epithelial cells to cytotoxic insults (Nguyen *et al.*, 2020). This idea is further supported by the finding that TRPV3 inhibition prevented increases in airway resistance in WSPM-treated mice, via an unknown mechanism (Deering-Rice *et al.*, 2018).

Downloaded from molpharm.aspetjournals.org at ASPET Journals on March 20, 2024

Molecular Pharmacology Fast Forward. Published on July 21, 2021 as DOI: 10.1124/molpharm.121.000280
This article has not been copyedited and formatted. The final version may differ from this version.

TRPV3 is important in cutaneous physiology and plays roles in pain, itch, hair growth, and skin homeostasis (Cheng *et al.*, 2010; Yang *et al.*, 2017). TRPV3 is necessary for regulated keratinocyte proliferation and the formation and maintenance of the skin barrier, including terminal differentiation of the epidermis (Borbíró *et al.*, 2011). Knock-out of *Trpv3* in mice reduces terminal differentiation and barrier integrity, and promotes a curly hair morphology, in part, by interactions with the TGFα/EGFR signaling nexus (Cheng *et al.*, 2010). There have been no pulmonary phenotypes associated with *Trpv3* knockout. Alternatively, low-level TRPV3 activation may stimulate cell growth, while over-stimulation of TRPV3 inhibits proliferation and induces apoptosis. Of note, the congenital disorder, Olmsted syndrome, is caused by rare mutations rendering TRPV3 constitutively active, leading to palmoplantar keratoderma, perioral keratotic plaques, and severe itching at lesions (Lin *et al.*, 2012). These morbidities can be attributed to the fragility of the epithelium, in which overgrowth of keratinocytes serves as protection, manifesting as hyperkeratosis (McLean and Irvine, 2007). Also, no pulmonary phenotypes have been associated with Olmsted syndrome.

TRPV3 may have similar roles in the lung epithelium. The airway epithelium is the first line of defense against environmental insults such as inhaled particles, pathogens and toxic chemicals, and it is a common site of damage by inhaled pneumotoxicants. Improper control of inflammation and resolution of repair can promote airway remodeling and adverse health outcomes (Zemans *et al.*, 2013). The initial stages of epithelial repair are crucial, and include de-differentiation, spreading, and proliferation of epithelial cells adjacent to the wound. Immediate changes in ATP, H_2O_2 and Ca^{2+} stimulates, in a spatially and temporally limited manner, the expression of genes needed for repair. Receptor tyrosine kinases are also activated by pre-existing and transcriptionally induced growth factors, and chemokines that signal surrounding cells to engage in the repair process (Cordeiro and Jacinto, 2013). Studies using different tissues have found that voltage-gated Ca^{2+} channels, including TRP channels,

Downloaded from molpharm.aspetjournals.org at ASPET Journals on March 20, 2024

Molecular Pharmacology Fast Forward. Published on July 21, 2021 as DOI: 10.1124/molpharm.121.000280
This article has not been copyedited and formatted. The final version may differ from this version.

become induced, and are critical in maintaining Ca^{2+} homeostasis (Cordeiro and Jacinto, 2013). For example, TRPC1 (Fabian *et al.*, 2008), TRPV2 (Monet *et al.*, 2009), TRPV4 (Fiorio Pla *et al.*, 2012; Martin *et al.*, 2012), TRPM7 (Middelbeek *et al.*, 2015) and TRPM8 (Wondergem and Bartley, 2009) regulate cell migration in various cell types. How TRPV3 responds to cell injury and influences epithelial repair in the lungs is not known.

Here, it was postulated that TRPV3 helps coordinate repair in HBECs. It is shown that synchronized expression of TRPV3 is essential for epithelial repair following WSPM-induced and other forms of injury *in vitro* and in mouse airways. The results provide new insights into mechanisms by which TRPV3 may regulate WSPM injury and highlight possibilities for using TRPV3 ligands to modulate lung injury and repair.

Materials and Methods:

Chemicals: Unless specified, chemicals were purchased from Sigma-Aldrich (St. Louis, MO). The inhibitors CP-724714 (ErbB2) and PD169316 (p38 MAPK) were purchased from Cayman Chemical (Ann Arbor, MI). AG-1478 (ErbB1/EGFR) was purchased from Selleckchem.com (Houston, TX). AZD 8931 (EGFR, ErbB2, ErbB3) was purchased from APExBIO (Houston, TX), and TWS119 (GSK3β) and SP600125 (JNK) from ChemCruz (Dallas, TX). Afatinib dimaleate (EGFR, ErbB2, ErbB4), IWP 2 (Porcupine), SB 431542 (TGFβRI) and ITD 1 (TGFβRII) were purchased from Tocris (Minneapolis, MN). Recombinant human heparin-binding EGF-like growth factor (HB-EGF), epigen (EPGN), neuregulin 1 (NRG1), amphiregulin (AREG), recombinant human transforming growth factor β-2 (TGFβ2) and recombinant human secreted frizzled related protein-1 (sFRP-1) were purchased from R&D Systems (Minneapolis, MN). Recombinant human transforming growth factor β-1 (TGFβ1) was purchased from Abcam (Cambridge, United Kingdom) and Wnt7a from PeproTech (Rocky Hill, NJ). All recombinant human proteins were reconstituted and stored according to supplier recommendations. The

Downloaded from molpharm.aspetjournals.org at ASPET Journals on March 20, 2024

Molecular Pharmacology Fast Forward. Published on July 21, 2021 as DOI: 10.1124/molpharm.121.000280
This article has not been copyedited and formatted. The final version may differ from this version.

TRPV3 antagonists 2-(5-trifluoromethyl-pyridine-2ylsulfanyl)-1-(8-methyl-3,4-dihydro-2H-quinolin-1-yl)-ethanone (referred to hereafter as 007) and (*S*)-(1-(3,4-Dichlorophenyl)cyclobutyl)(pyridin-2-yl)methanol (referred to hereafter as 008; also known as 5a (Gomtsyan *et al.*, 2016)) were synthesized as previously described (Deering-Rice *et al.*, 2014) by the University of Utah Synthetic and Medicinal Chemistry Core. The purified products were verified by mass spectrometry, ^{1}H-NMR, and ^{13}C-NMR.

Cells: HBEC3-KT cells (ATCC; Rockville, MD) (Delgado *et al.*, 2011) were grown in Airway Epithelial Basal Medium supplemented with Bronchial Epithelial Cell Growth Kit (ATCC; Rockville, MD). BEAS-2B cells (ATCC; Rockville, MD) were grown in LHC-9. Human TRPV3 overexpressing BEAS-2B cells (B2BV3OE) were generated as previously described (Deering-Rice *et al.*, 2018). All cells were cultured in a humidified incubator at 37°C with a 95% air:5% CO_2 atmosphere, and regularly passaged using trypsin before becoming 100% confluent.

In vitro injury models: Cells were injured using four different processes: 1) *Cell passaging injury* was performed by washing confluent cells with PBS, adding trypsin (TrypLE Express Enzyme (1X), ThermoFisher) and incubating at 37°C for 5 min, dislodging cells, and re-plating cells; 2) *trypsin injury* was performed by incubating cells with trypsin (TrypLE Express, Invitrogen; Carlsbad, CA) for 1 min, removal of the trypsin, and monitoring under a light microscope until the monolayer was disrupted (i.e., cells were slightly rounded, and cell-cell contacts were lost; ~3-5 minutes depending upon cell type) - fresh media was then added; 3) *mechanical injury* in the form of a "*scratch wound"* created using a grid pattern was made using a pipette tip, washed twice with PBS to remove the non-adherent cells, and adding fresh media; and 4) *cytotoxic injury* which involved treatment of monolayers with a cytotoxic (~50% cell death with 24h treatment) concentration of pine WSPM (0.076 mg/mL equivalent to 20 $\mu g/cm^2$), which also disrupts the monolayer. These methods were chosen for purposes of studying mechanisms

Downloaded from molpharm.aspetjournals.org at ASPET Journals on March 20, 2024

Molecular Pharmacology Fast Forward. Published on July 21, 2021 as DOI: 10.1124/molpharm.121.000280
This article has not been copyedited and formatted. The final version may differ from this version.

of WSPM injury, as well as to ascertain the relevance of findings in the context of a proteolytic mechanism of injury, as well as to simply understand how cells respond when attempting to reform a damaged epithelial layer.

Pine WSPM: Pine WSPM was generated as previously described(Deering-Rice *et al.*, 2018). Approximately 10 g of dry Austrian pine, collected from a tree growing in the Salt Lake Valley, was burned in a laboratory furnace. PM was collected using an Anderson cascade impactor, and fraction 7 (F7; PM size: 0.43-0.65 μm) was re-suspended in DMSO to an initial concentration of 115 mg/mL or 500 mg/mL for *in vitro* and *in vivo* experiments, respectively. Pine WSPM was diluted further to the final working concentration of 0.076 mg/mL (20 μg/cm^2 in the 6-well treatment plates) in cell culture media, and 0.5 mg/mL, diluted in saline, for treatment of animals at a final dose of 0.5 mg/kg, as described below.

Quantitative real-time PCR (qPCR): Total RNA was isolated from cells using the PureLink RNA Mini Kit (Invitrogen; Carlsbad, CA). For time course experiments, cells were subjected to cell passaging injury. Cells were typsinized, and ½ of the cells were immediately collected for the t=0 baseline time point. The remaining cells were plated in 6-well plates for temporal gene expression studies. cDNA was synthesized from 2 μg of total RNA using the ABI High Capacity cDNA Synthesis Kit with RNase inhibitor (Applied Biosystems, Foster City, CA). The samples were probed for human TRPV3 mRNA (Hs00376854_m1) using TaqMan probes (Applied Biosystems). TaqMan probes for HB-EGF (Hs00181813_m1), EPGN (Hs02385424), AREG (Hs00950669) NRG1 (Hs01101538_m1), TGFβ1 (Hs00998133_m1), TGFβ2 (Hs00234244_m1), Wnt7a (Hs011149990_m1), ErbB1 (Hs01076090_m1), ErbB2 (Hs01001580_m1), ErbB3 (Hs00176538_m1), TGFβRI (Hs00610320_m1), TGFβRII (Hs00234253_m1), and FZD5 (Hs00258278_s1) were also used. Analysis by qPCR was performed using a Life Technologies QuantStudio 6 Flex instrument. Values for relative gene

Downloaded from molpharm.aspetjournals.org at ASPET Journals on March 20, 2024

Molecular Pharmacology Fast Forward. Published on July 21, 2021 as DOI: 10.1124/molpharm.121.000280
This article has not been copyedited and formatted. The final version may differ from this version.

expression were normalized to the "*housekeeping gene*" β*2*-microglobulin (B2M, Hs00984230_m1), which exhibited stability across treatments, utilizing the ΔΔCT method.

Ca^{2+} Flux Assay: Cells were plated in a 96-well plate (10,000 cells/well) and grown for either 24h or 84h. TRPV3-dependent Ca^{2+} flux was measured using the Fluo-4 Direct assay kit (Invitrogen; Carlsbad, CA). Fluo-4AM was diluted in LHC-9 and the cells were loaded at room temperature (22-23ºC) as previously described (Deering-Rice *et al.*, 2011). Fluorescence micrographs were captured using the EVOS FL Auto microscope at 10X magnification with a GFP filter. After baseline fluorescence was captured, cells were treated with the TRPV3-selective agonist drofenine, prepared in LHC-9 medium (which contains 111.1 μM Ca^{2+}), at 3X concentration at room temperature. Images were captured immediately prior to treatment application and every 40s thereafter, for 160s. Following agonist treatment, cells were treated with the Ca^{2+} ionophore, ionomycin (10 μM final concentration) in LHC-9 to determine the maximum attainable response and for normalization of the agonist-induced response. The change in fluorescence (i.e., Ca^{2+} content) was further normalized to blank LHC-9 media and quantified using an Image-J-based software.

Kinetic scratch wound assays: Cells were plated at 25,000 cells/cm^2 and grown for 48h to 100% confluence on an ImageLock 96-well culture plate (Essen BioSciences, Ann Arbor, MI). Precision mechanical "*scratch wounds"* were made using the Incucyte WoundMaker 96-pin wound-making tool (Essen BioSciences). The cells were then washed 2x with PBS to remove the detached cells and then the desired treatments were added. Scratch wound closure images were captured at 1h intervals using an IncuCyte ZOOM real-time live cell imaging system, which was housed in a climate-controlled cell culture incubator. Wound confluence was measured as the percent of the initial gap that was covered by migrating cells, and parameters were set, and the image series analyzed, using IncuCyte ZOOM software.

Downloaded from molpharm.aspetjournals.org at ASPET Journals on March 20, 2024

Molecular Pharmacology Fast Forward. Published on July 21, 2021 as DOI: 10.1124/molpharm.121.000280
This article has not been copyedited and formatted. The final version may differ from this version.

RNA sequencing: Transcript profiling of BEAS-2B and B2BV3OE cells was performed by the High Throughput Genomics Core Facility at the Huntsman Cancer Institute, University of Utah, as described previously (Deering-Rice *et al.*, 2018). Briefly, BEAS-2B and B2BV3OE cells were plated in T-25 flasks and grown to 100% confluence before RNA isolation. RNA was isolated using RNeasy kit with on column DNase1 digestion (Qiagen). The Illumina TruSeq Stranded mRNA Sample Preparation kit was used to generate the library and the samples were analyzed using an Illumina HiSeq instrument (HCS v2.0.12 and RTA v1.17.21.3), with a 50-cycle single read sequence. Data were processed by the University of Utah Bioinformatics Core. The data presented in this publication have been deposited in NCBI's Gene Expression Omnibus (Edgar *et al.*, 2002) and are accessible through GEO Series accession number GSE109598.

Cell adhesion assay: BEAS-2B and B2BV3OE cells were passaged and plated at a density of 30,000 cells/cm^2 in a 96-well plate with fresh LHC-9 media and incubated for 2h. Non-adherent cells were removed with two PBS washes. CCK-8 viability reagent (Dojindo, Rockville, MD) was diluted to 8% in LHC-9 media and then added to the culture wells to quantify adherent cells. After 2h incubation time at 37°C, the absorbance at 450 nm was determined using a plate reader. The number of adherent cells was calculated by comparing absorbance values to a standard curve of known cell seeding density/cell number plated and measured after the 2h incubation (without washing).

Mice: Experimental procedures were approved by the University of Utah Institutional Animal Care and Use Committee. Mice were housed in a vivarium with 12h light-dark cycles and provided standard chow and water *ad libitum*. Male and female 6-8 weeks old C57BL/6 mice weighing 20-25 g were used for sub-acute saline, pine WSPM, and TRPV3 antagonist (007) exposures. Both male and female mice were used to address sex as a variable, and no

Downloaded from molpharm.aspetjournals.org at ASPET Journals on March 20, 2024

Molecular Pharmacology Fast Forward. Published on July 21, 2021 as DOI: 10.1124/molpharm.121.000280
This article has not been copyedited and formatted. The final version may differ from this version.

overt differences have been observed. Saline vehicle control or fresh pine WSPM (0.5 mg/kg in saline) was dosed via oropharyngeal aspiration (OPA) for a total of 3 times, every other day. After (24h) the third dose (day 6), mice were sacrificed and the respiratory tissues collected. Rationale for this dosing paradigm has been previously described in detail (Deering-Rice *et al.*, 2018). Mice were also injected i.p. with the TRPV3 antagonist 007 at 1 mg/kg diluted in saline from a stock in DMSO (final DMSO=1%) 1h prior to pine WSPM instillation. These mice were also co-treated with 007 (1 μM) diluted in the pine WSPM suspension or saline, via OPA, to ensure local inhibition of TRPV3 during the WSPM exposure. 24h after the 3rd dose, mice were euthanized, and the lungs were inflated and fixed with 10% neutral-buffered formalin (NBF) at a constant hydrostatic pressure of 25 cm H_2O. The left lobe of the lungs was dissected, mounted, sliced into serial 5 μm sections and stained with Trichrome for histological analysis by the University of Utah Research Histology Core. Lungs from additional mice within the same treatment groups were also inflated with RNAlater and stored at 4°C. The lungs were then micro-dissected, separating the upper airways (trachea and bronchi) from the smaller, lower airways and parenchymal tissue, and placed in TRIzol. The tissue was immediately homogenized and extracted with chloroform, before further processing of the aqueous phase using the PureLink RNA Mini Kit (Invitrogen; Carlsbad, CA) to isolate total RNA. cDNA was synthesized from 2 μg of total RNA using the ABI High Capacity cDNA Synthesis Kit with RNase inhibitor (Applied Biosystems, Foster City, CA). The samples were probed for mouse *Trpv3* mRNA (Mm00455003_m1) using TaqMan probes (Applied Biosystems). Analysis by qPCR was performed using a Life Technologies QuantStudio 6 Flex instrument. Values for relative gene expression were normalized to the "*housekeeping gene*" mouse glyceraldehyde-3-phosphate dehydrogenase mRNA (*Gapdh*, Mm99999915_g1), which exhibited stability across treatments, using the ΔΔCT method. Some studies also utilized *Trpv3-/-* C57BL/6J mice. These mice were purchased from Jackson laboratories and were maintained on site, as described above.

Downloaded from molpharm.aspetjournals.org at ASPET Journals on March 20, 2024

Molecular Pharmacology Fast Forward. Published on July 21, 2021 as DOI: 10.1124/molpharm.121.000280
This article has not been copyedited and formatted. The final version may differ from this version.

TRPV3-Knockout HBEC3-KT cells: The target sequence 5'-GCCGGATGTTGGAATCCAT-3' was cloned into pX459-pSpCas9-2A-mCherry V2.0 (modified from Addgene, pSpCas9(BB)-2A-Puro V2.0) to co-express Cas9-2A-mCherry protein and a guide RNA targeting TRPV3 at exon 2. This sequence introduced a premature stop codon in the TRPV3 gene. HBEC-3KT cells were transfected with this construct using FuGENE 6 transfection reagent (Promega) at a 2:1 ratio of reagent to DNA in 250 μL OptiMEM media. To isolate stably modified cells, the cells were cultured, trypsinized, and sorted by flow cytometry using a BD FACSAria, collecting the top 1% of mCherry-expressing cells. Cells were then cultured and subjected to FAC sorting for 5 subsequent passages, isolating the top 1% of mCherry-positive cells in each sort as single cells to be expanded. On-target editing in the final cell line was verified by the University of Utah Mutation Generation and Detection Core Facility using TIDE sequencing.

Statistical analysis: Values are represented as the mean ± SD unless stated otherwise. For comparisons between two groups, the unpaired t-test was used. One-way ANOVA with Dunnett's post-test was used for multiple comparisons, unless indicated otherwise. A p-value <0.05 was considered significant.

Results:

TRPV3 mRNA and protein/function increased in HBEC3-KT cells following multiple types of monolayer injury: TRPV3 mRNA was quantified following different types of monolayer injury (**Figure 1A**). Compared to the vehicle control, pine WSPM treatment increased TRPV3 expression ~20-fold ($p<0.0001$), similar to that previously reported for primary lobar HBECs treated with pine WSPM (Nguyen *et al.*, 2020). Likewise, cell passaging and trypsin digestion alone increased TRPV3 mRNA ~25- and 10-fold ($p<0.0001$), respectively, while scratch

Downloaded from molpharm.aspetjournals.org at ASPET Journals on March 20, 2024

Molecular Pharmacology Fast Forward. Published on July 21, 2021 as DOI: 10.1124/molpharm.121.000280
This article has not been copyedited and formatted. The final version may differ from this version.

wounded cells exhibited a ~4-fold increase in TRPV3 mRNA (p=0.0755). The relatively limited change in TRPV3 mRNA in the mechanical/scratch wound model was attributed to less uniform/widespread monolayer damage. **Supplemental Table 1** shows additional results for up-regulation of TRPV3 mRNA using these injury models on other immortalized and primary HBEC cell lines.

After passaging injury, TRPV3 mRNA levels spiked at 2h and again at 18h, but as the cells re-established monolayer integrity and became confluent at ~72h post plating, the levels of TRPV3 mRNA returned to baseline (**Figure 1B**). Differences in TRPV3 expression in relation to confluence was confirmed as changes in TRPV3-dependent Ca^{2+} flux, as a function of time after plating (**Figure 1C**), as well as western blotting (**Supplemental Figure 1**). Specifically, cells that were less confluent and actively proliferating (i.e., high TRPV3 mRNA expression; 24h post plating at ~20% confluence) exhibited greater responses to drofenine, a selective TRPV3 agonist (Deering-Rice *et al.*, 2014), compared to 100% confluent cells (i.e., low TRPV3 mRNA expression; 84h post-plating, p<0.0001). This same time-dependent change in mRNA expression was observed in BEAS-2B cells and to a much lesser extent in B2BV3OE cells (**Supplemental Figure 2**).

Rapid increases in TRPV3 transcription did not require new protein synthesis: HBEC3-KT cells were subjected to passaging injury and treated for 2h with either 100 nM cycloheximide (CHX; a protein synthesis inhibitor), or 50 μM actinomycin D (ActD), a potent transcription inhibitor (**Figure 2**). CHX treatment enhanced TRPV3 mRNA expression ~1.5-fold (p=0.001). As expected, ActD treatment prevented an increase in TRPV3 expression (p<0.0001).

Overexpression of TRPV3 slows migration and wound repair while promoting cell adhesion: **Figure 3A** summarizes wound repair results following a mechanical/scratch. Representative live cell microscopy images comparing the extent of wound repair at 45h are

Downloaded from molpharm.aspetjournals.org at ASPET Journals on March 20, 2024

Molecular Pharmacology Fast Forward. Published on July 21, 2021 as DOI: 10.1124/molpharm.121.000280
This article has not been copyedited and formatted. The final version may differ from this version.

shown in **Figure 3B**. These results show that stable overexpression of TRPV3 (B2BV3OE cells) interfered with the ability of cells (red line) to repair a scratch injury, with full repair occurring well after 48h. Conversely, BEAS-2B cells (black line) repaired scratch wounds within ~6h. A scratch mask (red) and confluent cell mask (teal) is overlaid on the images in Figure 3B, to highlight the marked differences in wound closure. Time-lapse videos are also included as **Movie S1**. In the movie it was also noted that B2BV3OE cells were less mobile than BEAS-2B cells, moving more as a cohesive unit rather than individual cells migrating throughout the wound site.

Regulated cell adhesion is necessary for wound repair; too little or too much alters migration and repair potential (Crosby and Waters, 2010). As shown in **Figures 3A, 3B**, and **Movie S1**, B2BV3OE cells remained mostly stationary following scratch wounding, and B2BV3OE cells were found to be more adherent within 2h of plating (**Figure 3C)**. To this end, it was also found that TRPV3OE cells expressed comparatively lower levels of the mesenchymal marker Vimentin, while having higher levels of expression of E-cadherin and F-actin (**Supplemental Figure 3**). Additionally, TRPV3KO cells were ~20% less adherent than normal HBEC3-KT cells in an adhesion assay (data not shown).

Transcriptomic comparisons of normal and TRPV3 overexpressing cells suggested integration of TRPV3 with canonical growth factor signaling pathways: Transcriptomic analysis (**Figure 4A)** revealed lower levels of transcripts for multiple growth factors related to EGFR/ErbB1-3 signaling, as well as Wnt7a and TGFβ1 in B2BV3OE cells, but negligible differences in ErbB1-3, TGFβRI and Frizzled-5 (FZD5, activated by Wnt7a) receptors. qPCR analysis was also performed to confirm the transcriptomic results (**Figures 4B and C**). As expected, EPGN, AREG, NRG1 HB-EGF and Wnt7a were all down-regulated in B2BV3OE cells. However, TGFβ2 was up-regulated. TGFβ1 appeared to be slightly lower in B2BV3OE cells, but the change was not statistically significant ($p>0.05$).

Downloaded from molpharm.aspetjournals.org at ASPET Journals on March 20, 2024

Molecular Pharmacology Fast Forward. Published on July 21, 2021 as DOI: 10.1124/molpharm.121.000280
This article has not been copyedited and formatted. The final version may differ from this version.

Supplemental growth factors partially rescued the scratch wound repair capacity of B2BV3OE cells: The attenuated wound repair observed for B2BV3OE, 24h post scratch injury, cells was partially rescued when the media was supplemented with the growth factors HB-EGF (1 ng/mL), AREG (10 ng/mL), TGFβ1 (100 ng/mL) and TGFβ2 (100 ng/mL) during a mechanical/scratch wound repair assay (**Figure 5**). Images of the corresponding scratch wounds at 0 and 24h following scratch and supplementation of growth factors can be found in **Supplemental Figure 4**.

Increased TRPV3 mRNA expression paralleled increases in mRNA for EGFR ligands following injury, which in turn stimulated TRPV3 transcription: Increases in the expression of HB-EGF, AREG, TGFβ1 and Wnt7a mRNA occurred rapidly, and peaked ~2-4h after injury (**Figure 6A**); EPGN, NRG1, and TGFβ2 followed the same pattern of expression (**Supplemental Figure 5**). As with TRPV3, growth factor mRNA expression also decreased over time as cells restored monolayer integrity and reached 100% confluence (i.e., the 72h time point). Recombinant human EGFR, TGFβ1, and Fz receptor ligands were tested for their ability to regulate TRPV3 expression. Conditioned media from confluent cells was used in these experiments to avoid the effect of growth factors present in fresh media. As shown in **Figure 6B**, TRPV3 mRNA increased in a dose-dependent manner due to HB-EGF, AREG, TGFβ1, and Wnt7a (as well as TGFβ2; **Supplemental Figure 5**) treatment, compared to the conditioned media control.

Inhibiting EGFR, Wnt, and TGFβ signaling prevented increases in TRPV3 mRNA expression following injury: HBEC3-KT cells were plated following passage injury in the presence of 5 μM of the following inhibitors: AG-1478 (EGFR/ErbB-1), AZD8931 (EGFR, ErbB2 and ErbB3), Afatinib (EGFR, ErbB2 and ErbB4) and CP-724 (ErbB2/HER2) (**Figure 7A**). CP-724 treatment had minimal effect on TRPV3 transcript levels while AG-1478, AZD8931 and

Downloaded from molpharm.aspetjournals.org at ASPET Journals on March 20, 2024

Molecular Pharmacology Fast Forward. Published on July 21, 2021 as DOI: 10.1124/molpharm.121.000280
This article has not been copyedited and formatted. The final version may differ from this version.

Afatinib treatment attenuated changes in TRPV3 mRNA expression by >60%, indicating that increases in TRPV3 expression occurred following EGFR/ErbB-1 activation, but seemingly not ErbB2, B3, or B4 activation. Although not shown, EGFR inhibition also prevented scratch wound repair by HBEC3-KT and BEAS-2B cells.

HBEC3-KT cells were also plated following passage injury in media fortified with either 10 μM SP600125 (JNK inhibitor), 10 μM PD169316 (p38 MAPK inhibitor), 20 μM CCT036477 (β-catenin inhibitor), 20 μM BMS-345541 (NF-κB inhibitor), or 5 μM TWS119 (GSK3β inhibitor). Inhibiting GSK3β, β-catenin, and p38 MAPK, as well as NF-κB all reduced TRPV3 mRNA abundance by ~60%, indicating a key role for these molecules and the EGFR network in regulating changes in TRPV3 expression (**Figure 7B and C**). Conversely, JNK inhibition slightly increased TRPV3 expression, suggesting that JNK may negatively regulate TRPV3 increased expression following injury.

Further, Wnt and TGFβ signaling were blocked with 10 ng/mL sFRP-1 (prevents Wnt activation of Fzd and canonical signaling), 25 μM IWP 2 (a Porcupine inhibitor, preventing the secretion of Wnt proteins), 100 μM SB 431542 (TGFβRI inhibitor) and 150 μM ITD-1 (TGFβRII inhibitor). TRPV3 up-regulation was reduced with each inhibitor, with the exception of ITD-1 (**Figure 7D**).

TRPV3 inhibition attenuated mouse airway remodeling following sub-acute oropharyngeal exposure to pine PM: *Trpv3* mRNA increased ~2.5-fold in the conducting airways of WSPM-treated mice (p=0.0214, **Figure 8A)**, but not in parenchymal tissue samples (**Supplementary Figure 6**) where we have also observed lower levels of TRPV3 expression in anatomically representative human cell lines (Deering-Rice *et al.*, 2018). Representative photomicrographs (40X) of trichrome-stained C57BL/6 mouse 1st generation bronchi are shown in **Figure 8B**. The epithelium of the bronchi of pine WSPM-treated mice exhibited a

Downloaded from molpharm.aspetjournals.org at ASPET Journals on March 20, 2024

Molecular Pharmacology Fast Forward. Published on July 21, 2021 as DOI: 10.1124/molpharm.121.000280
This article has not been copyedited and formatted. The final version may differ from this version.

disorganized epithelium characterized by a stratified layer of epithelial cells stained deep red, characteristic of keratinization; a disrupted basal lamina (collagen stained blue), and a loss of ciliated cells. These morphological anomalies were consistent with the reported effects of wood smoke PM in rabbits, sheep and humans (Thorning *et al.*, 1982; Barrow *et al.*, 1992; Jacob *et al.*, 2010), and were not observed in pine PM+007 co-treated mice or in the 007 only control group.

TRPV3 antagonists unexpectedly increased TRPV3 mRNA expression and attenuated HBEC migration/wound repair: It was found that several TRPV3 antagonists promoted TRPV3 mRNA expression and inhibited wound repair *in vitro* (**Figures 9A-F)**. Specifically, three structurally unique TRPV3 antagonists (i.e., 007, 008, and 2,2-diphenyltetrahydrofuran/DPTHF; **Figure 9A**), which effectively block TRPV3-mediated Ca^{2+} flux (Deering-Rice *et al.*, 2014, 2018; Nilius *et al.*, 2014), were studied. Surprisingly, when HBEC3-KT cells were treated with the TRPV3 antagonists, TRPV3 mRNA was up-regulated in excess of what occurred 2h post injury alone (**Figure 9B**). 008 had the strongest effect on the expression of TRPV3 ($p<0.0001$), and all three of the antagonists attenuated monolayer wound repair (**Fig. 9C-F**). Representative real-time microscopy images (10X) illustrating the extent of scratch wound repair at 48h are shown in **Figures 9E-F** and time lapse videos are included as **Movie S2** (007 and 008) and **Movie S3** (DPTHF).

TRPV3 knockout also promoted TRPV3 mRNA expression: As shown in **Table 1**, TRPV3KO HBEC3-KT cells expressed ~34-fold more mRNA for TRPV3 than the control cell line ($p=0.0002$). Elevated TRPV3 mRNA expression also persisted over the time course of repair following cell passage injury. Consistent with this finding, the basal level of mRNA expression in conducting airway tissue of *Trpv3-/-* mice treated with saline was, on average, ~100-fold greater than in normal C57BL/6 mice ($p=0.0073$)

Downloaded from molpharm.aspetjournals.org at ASPET Journals on March 20, 2024

Molecular Pharmacology Fast Forward. Published on July 21, 2021 as DOI: 10.1124/molpharm.121.000280
This article has not been copyedited and formatted. The final version may differ from this version.

Discussion:

This study shows that TRPV3 is dynamically expressed by HBECs and in mouse airways following injury, and this phenomenon plays a role in wound repair and restoration of epithelial homeostasis. Additionally, TRPV3 expression and function varied over the course of the monolayer repair process, and this dynamic expression of TRPV3 is required to effectively coordinate repair, since inhibition of TRPV3 expression using EGFR inhibitors, stable over-expression of TRPV3, and treating cells with TRPV3 antagonists all interfered with wound repair. The rapid increase in TRPV3 expression after monolayer injury, and a decrease at later stages of repair when cells became confluent, among other results, suggests there is an optimum level of TRPV3 expression at various stages of the repair cycle, regulated via crosstalk with traditional growth factor signaling networks that drive cell motility and proliferation.

Elevated TRPV3 expression and involvement in wound repair was previously reported by Aijima *et al*. where it was shown that TRPV3 mRNA was up-regulated 3 and 5 days post-molar tooth extraction in human oral epithelial tissue, and that *Trpv3* was necessary for healing of oral mucosa of mice (Aijima *et al.*, 2014). TRPV3 mRNA has also been shown to be up-regulated in keratinocytes from patients with hypertrophic post-burn scars, which correlated with increased TRPV3-specific Ca^{2+} flux (Kim *et al.*, 2016). Interestingly, the TRPV3 agonist carvacrol was found to stimulate corneal epithelial cell repair at low levels, while higher levels became inhibitory (Yamada *et al.*, 2010). These studies further support the concept that TRPV3 is both critical for coordinating wound repair, and that the level of TRPV3 expression and TRPV3 function is purposefully regulated by cells, to optimum levels, as a function of cell status.

Consistent with this idea, the capacity to rapidly increase TRPV3 expression in HBECs is basally present (**Figure 2**). Inhibition of transcription using ActD prevented TRPV3 up-regulation following injury, but inhibition of protein synthesis with CHX enhanced TRPV3 expression. These data seem to suggest the existence of a fundamental process regulating the

Downloaded from molpharm.aspetjournals.org at ASPET Journals on March 20, 2024

Molecular Pharmacology Fast Forward. Published on July 21, 2021 as DOI: 10.1124/molpharm.121.000280
This article has not been copyedited and formatted. The final version may differ from this version.

expression of TRPV3 upon cell injury in a context-specific manner, to achieve an optimum level of expression that is presumably regulated by TRPV3 activity. Elevated TRPV3 transcript levels due to CHX treatment is also consistent with studies showing CHX treatment up-regulates transcriptional activity and stabilizes mRNA, potentially through p38 MAPK and NF-κB (Hershko *et al.*, 2004), which were found here to regulate TRPV3 mRNA expression.

Shedding of growth factors that target EGFR/ErbB and other growth factor receptors affect Ca^{2+} dynamics (Bryant *et al.*, 2004), which regulates the injury repair cycle. TRPV3-mediated Ca^{2+} flux has been linked to increased phosphorylation of EGFR in repairing oral epithelial cells, whereas knocking out *Trpv3* in mice reduced phospho-EGFR, indicating coupling between TRPV3 and EGFR signaling (Aijima *et al.*, 2014). Further, TRPV3 activation has been linked to keratinocyte proliferation through the activation of EGFR (Wang *et al.*, 2020). Like TRPV3, increased expression of mRNA for several EGF ligands was observed almost immediately after HBEC monolayer injury, and HB-EGF and AREG treatment promoted TRPV3 mRNA expression. Thus, it is probable that the up-regulation of TRPV3 in HBECs by EGFR signaling serves to regulate Ca^{2+} dynamics within cells throughout the repair process. Furthermore, inhibition of downstream component proteins of the EGFR signaling cascade, including p38 MAPK, GSK3β, β-catenin and NF-κB participate in the regulation of TRPV3 expression.

Wnt and TGFβ signaling also regulate epithelial repair. The expression of Wnt7a, TGFβ1 and TGFβ2 expression also increased in HBECs following injury, and all three stimulated TRPV3 mRNA expression. Like EGFR, GSK3β and β-catenin are also involved in the Wnt signaling pathway (McCubrey *et al.*, 2014). Wnt-secreted proteins bind to Fz receptors to stabilize β-catenin, while translocation of β-catenin into the nucleus stimulates the transcription of Wnt target genes that facilitate development, differentiation and cell growth (Wang *et al.*,

Downloaded from molpharm.aspetjournals.org at ASPET Journals on March 20, 2024

Molecular Pharmacology Fast Forward. Published on July 21, 2021 as DOI: 10.1124/molpharm.121.000280
This article has not been copyedited and formatted. The final version may differ from this version.

2018). Additionally, TGFβ plays a role in cell repair. TGFβ isoforms bind to multiple receptors (i.e., TGFβRI, TGFβRII and TGFβRIII) to activate SMAD signaling and the expression of epithelial-to-mesenchymal transition (EMT) biomarkers, and other TGFβ-responsive genes that control differentiation and wound repair (Wendt *et al.*, 2009). Of particular relevance are the effects of TGFβ on cell adhesion. TGFβ1 expression has been previously associated with cell migration (Giehl and Menke, 2006), while TGFβ2 has been linked to proliferation and adhesion (Kennedy *et al.*, 2008). B2BV3OE cells were more adherent, while TRPV3KO cells were less adherent. Given that B2BV3OE cells express higher TGFβ2/TGFβRII and slightly lower TGFβ1/TGFβRI, it is likely that aberrant TGFβ signaling also contributed to the attenuated repair phenotype of B2BV3OE cells. Another interesting observation was that TGFβ2 and TGFβRII were expressed ~5.5- and 5.0-fold higher (respectively) in B2BV3OE cells. TGFβ2 supplementation has been found to arrest the cell cycle (Abraham *et al.*, 2018) and promote adhesion (Mytilinaiou *et al.*, 2013), while TGFβRII under-expression has been linked to proliferation and tumorigenesis. Conversely, TGFβRII overexpression has been associated with suppression of cell growth (Yang *et al.*, 2017), as observed for the B2BV3OE cells. Thus, TRPV3 also appears to communicate with the Wnt/Fz and TGFβ signaling pathways to influence cell adhesion, migration, and overall repair capacity.

Over-expression of TRPV3 in BEAS-2B cells also altered the expression of several EMT genes (**Supplementary Figure 3**). EMT is regulated by growth factor signaling and is a coordinated process in which cells down-regulate cell adhesion and cytoskeletal proteins to become migratory mesenchymal cells. Upon monolayer repair, cells then undergo the reverse process of mesenchymal-to-epithelial transition (MET) (Xu *et al.*, 2009). In adhesion assays, TRPV3 overexpressing cells were more adherent than BEAS-2B cells (**Figure 3C**), and immunocytochemical staining for epithelial adhesion markers showed that B2BV3OE cells

Downloaded from molpharm.aspetjournals.org at ASPET Journals on March 20, 2024

Molecular Pharmacology Fast Forward. Published on July 21, 2021 as DOI: 10.1124/molpharm.121.000280
This article has not been copyedited and formatted. The final version may differ from this version.

expressed more F-actin (an epithelial marker) compared to BEAS-2Bs (**Supplementary Figure 3**). These results suggest that TRPV3 specifically interacts with growth factor signaling pathways to alter their dynamics at basal (epithelial) and in dynamic (mesenchymal) states.

The integration of TRPV3 and growth factor signaling is consistent with a prior report by, Cheng *et. al.* who demonstrated a link between TRPV3, EGFR, and TGFα signaling; proposing that EGFR signaling activates TRPV3 located on the surface of skin keratinocytes to promote the release of TGFα (Cheng *et al.*, 2010). These authors postulated a "positive feedback loop" between TRPV3 and TGFα release. This mechanism is consistent with that proposed for TGFβ, Wnt7a, and EGFR ligands in this study, with the caveat that this study implies a negative feedback mechanism for EGFR, Wnt, and TGFβ signaling, as a function of TRPV3 expression/function. This feedback is presumably maintained through the regulation of Ca^{2+} concentrations between the ER and cytosol of actively repairing cells. Although TGFα signaling was not evaluated here, transcriptomic profiling revealed negligible changes (1.14-fold) in TGFα transcripts in the B2BV3OE cells compared to BEAS-2B cells. A schematic of the cell signaling pathways that affect TRPV3 expression, and *vice versa* is provided by **Figure 10**.

A goal of this study was to understand how variations in TRPV3 activity might affect lung injury in mice treated with WSPM. As shown, the bronchial airways of mice treated with WSPM exhibited morphological changes including epithelial hyperplasia, which likely underlies previous findings that WSPM treatment increased airway resistance in mice, which was inhibited by the TRPV3 antagonist 007 (Deering-Rice *et al.*, 2018). The effects of WSPM treatment are consistent with reports that low-level TRPV3 activation by agonists can promote cell growth (Yamada *et al.*, 2010), and prior reports of the effects of wood/biomass smoke on the airway epithelium of various species (Thorning *et al.*, 1982; Barrow *et al.*, 1992; Jacob *et al.*, 2010). However, in this work, we were unable to confirm a relationship between TRPV3 agonists and enhanced cell growth *in vitro* using HBECs or in mice, thus, we cannot rule out the possibility

Downloaded from molpharm.aspetjournals.org at ASPET Journals on March 20, 2024

Molecular Pharmacology Fast Forward. Published on July 21, 2021 as DOI: 10.1124/molpharm.121.000280
This article has not been copyedited and formatted. The final version may differ from this version.

that TRPV3 stimulation contributed to the epithelial changes associated with WSPM exposure in mice. However, the observation that TRPV3 antagonists promote TRPV3 expression by HBECs and prevent repair, as well as the finding that *Trpv3* knock-out increases *Trpv3* mRNA in mouse airways, supports the hypothesis that the protective effect of 007 on airway remodeling, may be the result of increased TRPV3 expression, mimicking the effects of TRPV3-overexpression in HBECs, as TRPV3 knock out in HBEC3-KT cells does not prevent epithelial repair. However, this paradigm requires further study.

To summarize, TRPV3 appears to be crucial in regulating airway epithelial cell repair, and the findings related to the alterations in TRPV3 expression and activity caused by various biochemical and pharmacological manipulations could have broad significance in the development of therapeutics and furthering our understanding of the pathogenesis of selected respiratory diseases.

Downloaded from molpharm.aspetjournals.org at ASPET Journals on March 20, 2024

Molecular Pharmacology Fast Forward. Published on July 21, 2021 as DOI: 10.1124/molpharm.121.000280
This article has not been copyedited and formatted. The final version may differ from this version.

Acknowledgments: None

Authorship Contributions:

Participated in research design: Burrell, Nguyen, Deering-Rice, Memon, Lamb, Reilly

Conducted experiments: Burrell, Nguyen, Deering-Rice, Memon, Almestica-Roberts, Rapp, Serna, Lamb, Reilly

Contributed new reagents or analytic tools: None

Performed data analysis: Burrell, Nguyen, Deering-Rice, Memon, Almestica-Roberts, Rapp, Reilly

Wrote or contributed to writing of the manuscript: Burrell, Nguyen, Deering-Rice, Memon, Almestica-Roberts, Reilly

Downloaded from molpharm.aspetjournals.org at ASPET Journals on March 20, 2024

Molecular Pharmacology Fast Forward. Published on July 21, 2021 as DOI: 10.1124/molpharm.121.000280
This article has not been copyedited and formatted. The final version may differ from this version.

References:

Abraham CG, Ludwig MP, Andrysik Z, Pandey A, Joshi M, Galbraith MD, Sullivan KD, and Espinosa JM (2018) ΔNp63α Suppresses TGFB2 Expression and RHOA Activity to Drive Cell Proliferation in Squamous Cell Carcinomas. *Cell Rep* **24**:3224–3236.

Aijima R, Wang B, Takao T, Mihara H, Kashio M, Ohsaki Y, Zhang J-Q, Mizuno A, Suzuki M, Yamashita Y, Masuko S, Goto M, Tominaga M, and Kido MA (2014) The thermosensitive TRPV3 channel contributes to rapid wound healing in oral epithelia. *FASEB J* **29**:182–192, Federation of American Societies for Experimental Biology.

Barrow RE, Wang C-Z, Cox RA, and Evans MJ (1992) Cellular sequence of tracheal repair in sheep after smoke inhalation injury. *Lung* **170**:331–338.

Borbíró I, Lisztes E, Tóth BI, Czifra G, Oláh A, Szöllősi AG, Szentandrássy N, Nánási PP, Péter Z, Paus R, Kovács L, and Bíró T (2011) Activation of Transient Receptor Potential Vanilloid-3 Inhibits Human Hair Growth. *J Invest Dermatol* **131**:1605–1614.

Bryant JA, Finn RS, Slamon DJ, Cloughesy TF, and Charles AC (2004) EGF activates intracellular and intercellular calcium signaling by distinct pathways in tumor cells. *Cancer Biol Ther* **3**:1243–1249, Taylor & Francis.

Cheng X, Jin J, Hu L, Shen D, Dong X, Samie MA, Knoff J, Eisinger B, Liu M, Huang SM, Caterina MJ, Dempsey P, Michael LE, Dlugosz AA, Andrews NC, Clapham DE, and Xu H (2010) TRP Channel Regulates EGFR Signaling in Hair Morphogenesis and Skin Barrier Formation. *Cell* **141**:331–343.

Cordeiro J V, and Jacinto A (2013) The role of transcription-independent damage signals in the initiation of epithelial wound healing. *Nat Rev Mol Cell Biol* **14**:249–262.

Crosby LM, and Waters CM (2010) Epithelial repair mechanisms in the lung. *Am J Physiol Cell*

Downloaded from molpharm.aspetjournals.org at ASPET Journals on March 20, 2024

Molecular Pharmacology Fast Forward. Published on July 21, 2021 as DOI: 10.1124/molpharm.121.000280
This article has not been copyedited and formatted. The final version may differ from this version.

Mol Physiol **298**:L715–L731, American Physiological Society.

Deering-Rice CE, Memon T, Lu Z, Romero EG, Cox J, Taylor-Clark T, Veranth JM, and Reilly CA (2019) Differential Activation of TRPA1 by Diesel Exhaust Particles: Relationships between Chemical Composition, Potency, and Lung Toxicity. *Chem Res Toxicol* **32**:1040–1050, American Chemical Society.

Deering-Rice CE, Mitchell VK, Romero EG, Abdel Aziz MH, Ryskamp DA, Križaj D, Venkat RG, and Reilly CA (2014) Drofenine: a 2-APB analog with improved selectivity for human TRPV3. *Pharmacol Res Perspect* **2**:e00062, John Wiley & Sons, Ltd.

Deering-Rice CE, Nguyen N, Lu Z, Cox JE, Shapiro D, Romero EG, Mitchell VK, Burrell KL, Veranth JM, and Reilly CA (2018) Activation of TRPV3 by Wood Smoke Particles and Roles in Pneumotoxicity. *Chem Res Toxicol* **31**:291–301, American Chemical Society.

Deering-Rice CE, Romero EG, Shapiro D, Hughen RW, Light AR, Yost GS, Veranth JM, and Reilly CA (2011) Electrophilic Components of Diesel Exhaust Particles (DEP) Activate Transient Receptor Potential Ankyrin-1 (TRPA1): A Probable Mechanism of Acute Pulmonary Toxicity for DEP. *Chem Res Toxicol* **24**:950–959, American Chemical Society.

Delgado O, Kaisani AA, Spinola M, Xie X-J, Batten KG, Minna JD, Wright WE, and Shay JW (2011) Multipotent Capacity of Immortalized Human Bronchial Epithelial Cells. *PLoS One* **6**:e22023, Public Library of Science.

Edgar R, Domrachev M, and Lash AE (2002) Gene Expression Omnibus: NCBI gene expression and hybridization array data repository. *Nucleic Acids Res* **30**:207–210.

Fabian A, Fortmann T, Dieterich P, Riethmüller C, Schön P, Mally S, Nilius B, and Schwab A (2008) TRPC1 channels regulate directionality of migrating cells. *Pflügers Arch - Eur J Physiol* **457**:475.

Downloaded from molpharm.aspetjournals.org at ASPET Journals on March 20, 2024

Molecular Pharmacology Fast Forward. Published on July 21, 2021 as DOI: 10.1124/molpharm.121.000280
This article has not been copyedited and formatted. The final version may differ from this version.

Fiorio Pla A, Ong HL, Cheng KT, Brossa A, Bussolati B, Lockwich T, Paria B, Munaron L, and Ambudkar IS (2012) TRPV4 mediates tumor-derived endothelial cell migration via arachidonic acid-activated actin remodeling. *Oncogene* **31**:200–212.

Ghio AJ, Soukup JM, Case M, Dailey LA, Richards J, Berntsen J, Devlin RB, Stone S, and Rappold A (2012) Exposure to wood smoke particles produces inflammation in healthy volunteers. *Occup Environ Med* **69**:170 LP – 175.

Giehl K, and Menke A (2006) Moving on: Molecular mechanisms in TGFβ-induced epithelial cell migration. *Signal Transduct* **6**:355–364, John Wiley & Sons, Ltd.

Gomtsyan A, Schmidt RG, Bayburt EK, Gfesser GA, Voight EA, Daanen JF, Schmidt DL, Cowart MD, Liu H, Altenbach RJ, Kort ME, Clapham B, Cox PB, Shrestha A, Henry R, Whittern DN, Reilly RM, Puttfarcken PS, Brederson J-D, Song P, Li B, Huang SM, McDonald HA, Neelands TR, McGaraughty SP, Gauvin DM, Joshi SK, Banfor PN, Segreti JA, Shebley M, Faltynek CR, Dart MJ, and Kym PR (2016) Synthesis and Pharmacology of (Pyridin-2-yl)methanol Derivatives as Novel and Selective Transient Receptor Potential Vanilloid 3 Antagonists. *J Med Chem* **59**:4926–4947, American Chemical Society.

Hershko DD, Robb BW, Wray CJ, Luo G, and Hasselgren P-O (2004) Superinduction of IL-6 by cycloheximide is associated with mRNA stabilization and sustained activation of p38 map kinase and NF-κB in cultured caco-2 cells. *J Cell Biochem* **91**:951–961, John Wiley & Sons, Ltd.

Jacob S, Kraft R, Zhu Y, Jacob RK, Herndon DN, Traber DL, Hawkins HK, and Cox RA (2010) Acute secretory cell toxicity and epithelial exfoliation after smoke inhalation injury in sheep: An electron and light microscopic study. *Toxicol Mech Methods* **20**:504–509, Taylor & Francis.

Downloaded from molpharm.aspetjournals.org at ASPET Journals on March 20, 2024

Molecular Pharmacology Fast Forward. Published on July 21, 2021 as DOI: 10.1124/molpharm.121.000280
This article has not been copyedited and formatted. The final version may differ from this version.

Kennedy L, Shi-wen X, Carter DE, Abraham DJ, and Leask A (2008) Fibroblast adhesion results in the induction of a matrix remodeling gene expression program. *Matrix Biol* **27**:274–281.

Kim HO, Cho YS, Park SY, Kwak IS, Choi MG, Chung BY, Park CW, and Lee JY (2016) Increased activity of TRPV3 in keratinocytes in hypertrophic burn scars with postburn pruritus. *Wound Repair Regen* **24**:841–850, John Wiley & Sons, Ltd (10.1111).

Laumbach RJ, and Kipen HM (2012) Respiratory health effects of air pollution: update on biomass smoke and traffic pollution. *J Allergy Clin Immunol* **129**:3.

Lin Z, Chen Q, Lee M, Cao X, Zhang J, Ma D, Chen L, Hu X, Wang H, Wang X, Zhang P, Liu X, Guan L, Tang Y, Yang H, Tu P, Bu D, Zhu X, Wang K, Li R, and Yang Y (2012) Exome Sequencing Reveals Mutations in TRPV3 as a Cause of Olmsted Syndrome. *Am J Hum Genet* **90**:558–564.

Liu Sha, Zhou Y, Liu Suixin, Chen X, Zou W, Zhao D, Li X, Pu J, Huang L, Chen J, Li B, Liu Shiliang, and Ran P (2017) Association between exposure to ambient particulate matter and chronic obstructive pulmonary disease: results from a cross-sectional study in China. *Thorax* **72**:788 LP – 795.

Martin E, Dahan D, Cardouat G, Gillibert-Duplantier J, Marthan R, Savineau J-P, and Ducret T (2012) Involvement of TRPV1 and TRPV4 channels in migration of rat pulmonary arterial smooth muscle cells. *Pflügers Arch - Eur J Physiol* **464**:261–272.

McCubrey JA, Steelman LS, Bertrand FE, Davis NM, Sokolosky M, Abrams SL, Montalto G, D'Assoro AB, Libra M, Nicoletti F, Maestro R, Basecke J, Rakus D, Gizak A, Demidenko ZN, Cocco L, Martelli AM, and Cervello M (2014) GSK-3 as potential target for therapeutic intervention in cancer. *Oncotarget* **5**:2881–2911, Impact Journals LLC.

McLean WHI, and Irvine AD (2007) Disorders of keratinisation: from rare to common genetic

Downloaded from molpharm.aspetjournals.org at ASPET Journals on March 20, 2024

Molecular Pharmacology Fast Forward. Published on July 21, 2021 as DOI: 10.1124/molpharm.121.000280
This article has not been copyedited and formatted. The final version may differ from this version.

diseases of skin and other epithelial tissues. *Ulster Med J* **76**:72–82, The Ulster Medical Society.

Memon TA, Nguyen ND, Burrell KL, Scott AF, Almestica-Roberts M, Rapp E, Deering-Rice CE, and Reilly CA (2020) Wood Smoke Particles Stimulate MUC5AC Overproduction by Human Bronchial Epithelial Cells Through TRPA1 and EGFR Signaling. *Toxicol Sci* **174**:278–290.

Middelbeek J, Visser D, Henneman L, Kamermans A, Kuipers AJ, Hoogerbrugge PM, Jalink K, and van Leeuwen FN (2015) TRPM7 maintains progenitor-like features of neuroblastoma cells: implications for metastasis formation. *Oncotarget* **6**:8760–8776, Impact Journals LLC.

Monet M, Gkika D, Lehen'kyi V, Pourtier A, Abeele F Vanden, Bidaux G, Juvin V, Rassendren F, Humez S, and Prevarsakaya N (2009) Lysophospholipids stimulate prostate cancer cell migration via TRPV2 channel activation. *Biochim Biophys Acta - Mol Cell Res* **1793**:528–539.

Mytilinaiou M, Bano A, Nikitovic D, Berdiaki A, Voudouri K, Kalogeraki A, Karamanos NK, and Tzanakakis GN (2013) Syndecan-2 is a key regulator of transforming growth factor beta 2/Smad2-mediated adhesion in fibrosarcoma cells. *IUBMB Life* **65**:134–143, England.

Nguyen ND, Memon TA, Burrell KL, Almestica-Roberts M, Rapp E, Sun L, Scott AF, Rower JE, Deering-Rice CE, and Reilly CA (2020) Transient Receptor Potential Ankyrin-1 and Vanilloid-3 Differentially Regulate Endoplasmic Reticulum Stress and Cytotoxicity in Human Lung Epithelial Cells After Pneumotoxic Wood Smoke Particle Exposure. *Mol Pharmacol* **98**:586–597.

Nilius B, Bíró T, and Owsianik G (2014) TRPV3: time to decipher a poorly understood family member! *J Physiol* **592**:295–304, John Wiley & Sons, Ltd (10.1111).

Downloaded from molpharm.aspetjournals.org at ASPET Journals on March 20, 2024

Molecular Pharmacology Fast Forward. Published on July 21, 2021 as DOI: 10.1124/molpharm.121.000280
This article has not been copyedited and formatted. The final version may differ from this version.

Olloquequi J, and Silva O R (2016) Biomass smoke as a risk factor for chronic obstructive pulmonary disease: effects on innate immunity. *Innate Immun* **22**:373–381, SAGE Publications Ltd STM.

Reid CE, Michael B, Johnston FH, Jerrett M, Balmes JR, and Elliott CT (2016) Critical Review of Health Impacts of Wildfire Smoke Exposure. *Environ Health Perspect* **124**:1334–1343, Environmental Health Perspectives.

Shapiro D, Deering-Rice CE, Romero EG, Hughen RW, Light AR, Veranth JM, and Reilly CA (2013) Activation of Transient Receptor Potential Ankyrin-1 (TRPA1) in Lung Cells by Wood Smoke Particulate Material. *Chem Res Toxicol* **26**:750–758, American Chemical Society.

Swiston JR, Davidson W, Attridge S, Li GT, Brauer M, and van Eeden SF (2008) Wood smoke exposure induces a pulmonary and systemic inflammatory response in firefighters. *Eur Respir J* **32**:129 LP – 138.

Thorning DR, Howard ML, Hudson LD, and Schumacher RL (1982) Pulmonary responses to smoke inhalation: Morphologic changes in rabbits exposed to pine wood smoke. *Hum Pathol* **13**:355–364.

Wang Y, Li H, Xue C, Chen H, Xue Y, Zhao F, Zhu MX, and Cao Z (2020) TRPV3 enhances skin keratinocyte proliferation through EGFR-dependent signaling pathways. *Cell Biol Toxicol*, doi: 10.1007/s10565-020-09536-2.

Wang Z, Li R, He Y, and Huang S (2018) Effects of secreted frizzled-related protein 1 on proliferation, migration, invasion, and apoptosis of colorectal cancer cells. *Cancer Cell Int* **18**:48.

Wendt MK, Allington TM, and Schiemann WP (2009) Mechanisms of the epithelial-

Downloaded from molpharm.aspetjournals.org at ASPET Journals on March 20, 2024

Molecular Pharmacology Fast Forward. Published on July 21, 2021 as DOI: 10.1124/molpharm.121.000280
This article has not been copyedited and formatted. The final version may differ from this version.

mesenchymal transition by TGF-beta. *Future Oncol* **5**:1145–1168.

Wondergem R, and Bartley JW (2009) Menthol increases human glioblastoma intracellular Ca2+, BK channel activity and cell migration. *J Biomed Sci* **16**:90, BioMed Central.

Xu J, Lamouille S, and Derynck R (2009) TGF-β-induced epithelial to mesenchymal transition. *Cell Res* **19**:156–172.

Yamada T, Ueda T, Ugawa S, Ishida Y, Imayasu M, Koyama S, and Shimada S (2010) Functional expression of transient receptor potential vanilloid 3 (TRPV3) in corneal epithelial cells: Involvement in thermosensation and wound healing. *Exp Eye Res* **90**:121–129.

Yang H, Zhang H, Zhong Y, Wang Q, Yang L, Kang H, Gao X, Yu H, Xie C, Zhou F, and Zhou Y (2017) Concomitant underexpression of TGFBR2 and overexpression of hTERT are associated with poor prognosis in cervical cancer. *Sci Rep* **7**:41670.

Zemans RL, McClendon J, Aschner Y, Briones N, Young SK, Lau LF, Kahn M, and Downey GP (2013) Role of β-catenin-regulated CCN matricellular proteins in epithelial repair after inflammatory lung injury. *Am J Physiol Cell Mol Physiol* **304**:L415–L427, American Physiological Society.

Downloaded from molpharm.aspetjournals.org at ASPET Journals on March 20, 2024

Molecular Pharmacology Fast Forward. Published on July 21, 2021 as DOI: 10.1124/molpharm.121.000280
This article has not been copyedited and formatted. The final version may differ from this version.

Footnotes:

This work was supported by National Institute of Environmental Health Sciences (NIEHS) grants [ES017431] and [ES027015]. Katherine L. Burrell received partial support from a University of Utah Associated Regional and University Pathologists (ARUP) fellowship and the Skaggs Graduate Research Fellowship. Nam D. Nguyen was supported in part by a University of Utah Undergraduate Opportunities award, and Marysol Almestica-Roberts by a National Institute of General Medical Sciences (NIGMS) Diversity Supplement award associated with grant [GM121648]. Histological slide processing and staining was performed at the Research Histology Core Facility, a part of ARUP laboratories, at the Huntsman Cancer Institute, University of Utah. Transcript profiling of BEAS-2B and B2BV3OE cells was performed by the High Throughput Genomics Core Facility at the Huntsman Cancer Institute, University of Utah. The authors declare no conflicts of interest.

Downloaded from molpharm.aspetjournals.org at ASPET Journals on March 20, 2024

Molecular Pharmacology Fast Forward. Published on July 21, 2021 as DOI: 10.1124/molpharm.121.000280
This article has not been copyedited and formatted. The final version may differ from this version.

Figure Legends:

Figure 1. TRPV3 expression increased following epithelial injury *in vitro.* A) TRPV3 expression in HBEC3-KT cells after four different *in vitro* models of barrier disruption: 0.076 mg/mL pine PM for 2h, disruption of the monolayer by cell passaging, limited trypsin digestion, or mechanical/scratch wounding. **B)** Kinetics of TRPV3 mRNA expression following cell passaging injury (left y-axis). The grey fill (right y-axis) represents cell confluence. Data were normalized to 0h, non-injured control cells and are presented as the mean ± SD from $n \geq 3$ replicates. Statistical significance was determined using one-way ANOVA with the Dunnett post-test *$p < 0.05$, **$p < 0.01$, ***$p < 0.001$, ****$p < 0.0001$. **C)** Ca^{2+} flux assay using the TRPV3 agonist drofenine in HBEC3-KTs cultured for 24h post plating (~20% confluence; white) or 84h (100% confluent; grey). Data are presented as mean ± SD from $n \geq 3$ replicates and statistical significance was determined using two-way ANOVA with the post-hoc Sidak test ****$p < 0.0001$.

Figure 2. Effects of transcriptional and translational inhibitors on TRPV3 mRNA expression following epithelial injury *in vitro.* TRPV3 expression in HBEC3-KT cells was measured 2h after passaging injury, with and without treatment with 50 µM Actinomycin D (ActD, a transcriptional inhibitor) or 100 nM cycloheximide (CHX; a protein synthesis inhibitor). Statistical significance was determined using one-way ANOVA with Dunnett's post-test ***$p < 0.001$, ****$p < 0.0001$.

Figure 3. Stable over-expression of TRPV3 in BEAS-2B HBECs attenuated cell migration and mechanical/scratch wound repair, while increasing cell adhesion. A) BEAS-2B cells (black line) repaired scratch wounds within 6h, while TRPV3-overexpressing BEAS-2B cells (B2BV3OE, red line) required >48h. Data are shown as the mean ± SD (dotted lines) from $n = 4$

Downloaded from molpharm.aspetjournals.org at ASPET Journals on March 20, 2024

Molecular Pharmacology Fast Forward. Published on July 21, 2021 as DOI: 10.1124/molpharm.121.000280
This article has not been copyedited and formatted. The final version may differ from this version.

replicates. **B)** Live-cell microscopy images (10X) of BEAS-2B and B2BV3OE cells 1 and 40h post-scratch, with a scratch mask (red) and cell confluence mask (teal) overlaid. Videos of the entire wound repair assay are included as **Movie S1**. **C)** Adhesion assay comparing BEAS-2B (black) to B2BV3OE (grey) cells. Data are shown as the mean ± SD from n = 8 replicates. Statistical significance was determined using an unpaired t test. ****p < 0.0001.

Figure 4. Stable overexpression of TRPV3 in BEAS-2B HBECs decreased mRNA expression for multiple EGFR ligands and other canonical growth factor signaling molecules. A) Log ratio/mean average (MA) plot of mRNA sequencing results comparing BEAS-2B and B2BV3OE cells. TRPV3 (green), the growth factors HB-EGF, AREG, NRG1, EPGN, EREG, TGFβ1, TGFβ2 and Wnt7a (red), and corresponding growth factor receptors (black) are highlighted. **B)** Quantitative analysis of mRNA expression for EREG, EPGN, AREG, NRG1, HB-EGF Wnt7a, TGFβ1 and TGFβ2 in confluent B2BV3OE cells. Data were normalized to confluent BEAS-2B cells and shown as the mean ± SD from *n* = 3 replicates. Statistical testing was performed using two-way ANOVA with the post-hoc Sidak test. **p*>0.05, ***p* < 0.01, ****p* < 0.001, *****p* < 0.0001. **C)** Expression of receptors EGFR (ErbB1), ErbB2, ErbB3, FZD5, TGFβRI and TGFβRII in confluent B2BV3OE cells compared to confluent BEAS-2B cells. Data are shown as the mean ± SD from *n* = 3 replicates performed using two-way ANOVA with the post-hoc Sidak test. *****p* < 0.0001.

Figure 5. Addition of down-regulated growth factors to TRPV3-overexpressing cells partially rescued the repair deficiency phenotype. Supplementation of B2BV3OE cells with 1 ng/mL HB-EGF, 10 ng/mL AREG, 100 ng/mL TGFβ1 and 100 ng/mL TGFβ2, in growth media, increased wound confluence during scratch wound repair compared to vehicle control

Downloaded from molpharm.aspetjournals.org at ASPET Journals on March 20, 2024

Molecular Pharmacology Fast Forward. Published on July 21, 2021 as DOI: 10.1124/molpharm.121.000280
This article has not been copyedited and formatted. The final version may differ from this version.

B2BV3OE cells at 24h. Images of scratches after 24h are shown in **Supplemental Figure 4**. Statistical significance was determined using one-way ANOVA with the Dunnett post-test. ** $p < 0.01$, *** $p < 0.001$, **** $p < 0.0001$.

Figure 6. Changes in EGFR, TGFβ and Fz receptor ligand expression post-passaging injury, and TRPV3 up-regulation by EGFR, TGFβ and Fz receptor ligand supplementation. **A)** Time-dependent up-regulation of HB-EGF, AREG, TGFβ1, and Wnt7a mRNA in HBEC3-KT cells compared to 0h confluent, non-injured control cells. **B)** TRPV3 mRNA expression 2h post-passaging injury with and without HB-EGF, AREG, TGFβ1, and Wnt7a supplementation of conditioned media. Data were normalized to 0h, non-injured cells and presented as mean ± SD from $n \geq 3$ replicates. Statistical significance was determined using one-way ANOVA with the Dunnett post-test. * $p < 0.05$, ** $p < 0.01$, *** $p < 0.001$, **** $p < 0.0001$.

Figure 7. Inhibition of EGFR and growth factor pathway components prevented TRPV3 mRNA up-regulation following injury. A) HBEC3-KT cells were treated with 5 μM solutions of inhibitors of multiple ErbB receptor tyrosine kinase isoforms: ErbB1 (EGFR) – specific inhibitor AG-1478, ErbB pan-inhibitors AZD8931 and Afatinib, and a selective ErbB2 (HER2) inhibitor CP-724 for 2h in the cell passaging injury model, followed by analysis of TRPV3 mRNA. **B)** Downstream targets of EGFR activation were also inhibited and TRPV3 expression was subsequently measured 2h following cell passaging injury. Inhibitors included 5 μM TWS119 (GSK3β), 20 μM CCT036477 (β-Catenin), 10 μM PD169316 (p38 MAPK), and 10 μM SP600125 (JNK). **C)** Inhibition of NF-κB (20 μM BMS-345541) and effects on TRPV3 mRNA 2h after cell passaging injury. **D)** Inhibitors of Wnt7a and Fzd signaling were also used: 10 ng/mL sFRP and IWP 2 (Porcupine inhibitor) reduced TRPV3 up-regulation following injury.

Downloaded from molpharm.aspetjournals.org at ASPET Journals on March 20, 2024

Molecular Pharmacology Fast Forward. Published on July 21, 2021 as DOI: 10.1124/molpharm.121.000280
This article has not been copyedited and formatted. The final version may differ from this version.

Furthermore, SB 431542 (TGFβRI inhibitor) and 150 μM ITD-1 (TGFβRII inhibitor) were also tested, and SB 431542 treatment prevented TRPV3 expression as well. Values were normalized to vehicle controls and are presented as mean ± SD from $n \geq 3$ replicates. Statistical significance was determined using one-way ANOVA with the Dunnett post-test. ***$p < 0.001$, ****$p < 0.0001$. For Figure 4C, an unpaired t-test was used. ****p<0.0001.

Figure 8. Remodeling of, and *Trpv3* mRNA up-regulation in the airways of mice treated with pine PM. A) *Trpv3* mRNA expression in upper/conducting airway tissue isolated from C57BL/6 mice treated with sub-acute dosing of 0.5 mg/kg pine PM via OPA. Data represent the mean ± SD from n ≥ 3 for each treatment and statistical significance was determined using an unpaired t-test. *$p < 0.05$. **B)** Representative photomicrographs (40X) of trichrome-stained C57BL/6 mouse 1st generation bronchial epithelium following OPA of saline or 0.5 mg/kg pine PM with and without TRPV3 antagonist (007) pre- (1 mg/kg i.p., 1h prior) and co-treatment (1 μM OPA). The red arrow highlights remodeled epithelium suggestive of keratinization and epithelial hyperplasia.

Figure 9. Structurally unique TRPV3 antagonists increased TRPV3 mRNA expression in HBECs and slowed wound repair. A) Chemical structures of the TRPV3 antagonists 008, 007 and 2,2-diphenyltetrahydrofuran (DPTHF). **B)** TRPV3 mRNA expression was increased in confluent HBEC3-KT cells following 2h treatment with multiple TRPV3 antagonists. Data were normalized to vehicle controls and are presented as the mean ± SD from $n \geq 3$ replicates. Statistical significance was determined using one-way ANOVA with the Dunnett post-test. **p < 0.01, ****p < 0.0001. Scratch wound repair of HBEC3-KT cells treated with **C)** 007 (teal line) or 008 (green line) and **D)** DPTHF (red line) compared to untreated controls (black lines). Growth

Downloaded from molpharm.aspetjournals.org at ASPET Journals on March 20, 2024

Molecular Pharmacology Fast Forward. Published on July 21, 2021 as DOI: 10.1124/molpharm.121.000280
This article has not been copyedited and formatted. The final version may differ from this version.

curves are shown as the mean ± SD (dotted line) from *n* = 3 replicates. Live-cell microscopy images (10X) of vehicle versus **E)** 300 μM 008 treated cells, and **F)** DPTHF treated cells, 0 and 48h post-scratch. A scratch mask (red) and confluence mask (teal) are overlaid. Videos of the antagonist effect on wound repair are included as **Movie S2** (008 and 007) and **Movie S3** (DPTHF).

Figure 10. Summary schematic of cell signaling pathways that influence, and in turn are influenced by, TRPV3 activity and expression within lung epithelial cells following simulated epithelial injury. Components tested in this study are highlighted as red text. EGFR ligands, TGFβ and Wnt signaling factors activate signaling cascades including p38 MAPK, NF-κB, GSK3β and β-catenin to affect TRPV3 expression following injury. It is further suggested that TRPV3 expression and activity in turn affect growth factor expression and shedding to slow repair and to restore proper epithelial homeostasis following injury repair.

Downloaded from molpharm.aspetjournals.org at ASPET Journals on March 20, 2024

Molecular Pharmacology Fast Forward. Published on July 21, 2021 as DOI: 10.1124/molpharm.121.000280
This article has not been copyedited and formatted. The final version may differ from this version.

Table 1: Elevated TRPV3 mRNA expression in TRPV3KO HBEC3-KT and conducting airway tissue of *Trpv3-/-* mice.

Model Identity	**TRPV3 mRNA (Fold Control)**
HBEC-3KT cells	1.00 ± 0.03
TRPV3KO HBEC3-KT cells	34 ± 7***
C57BL/6 mice	1.2 ± 0.8
Trpv3-/- C57BL/6 mice	110 ± 54**

TRPV3 mRNA expression in HBECs is normalized to the HBEC3-KT control and presented as the mean ± SD from n = 4 replicates. Statistical significance was determined using an un-paired t-test (***p<0.001). *Trpv3* mRNA expression in mouse lung tissue is normalized to the C57BL/6 control and presented as the mean ± SD from n ≥ 4 replicates. Statistical significance was determined using an unpaired t-test (**p<0.01).

Downloaded from molpharm.aspetjournals.org at ASPET Journals on March 20, 2024

Molecular Pharmacology Fast Forward. Published on July 21, 2021 as DOI: 10.1124/molpharm.121.000280
This article has not been copyedited and formatted. The final version may differ from this version.

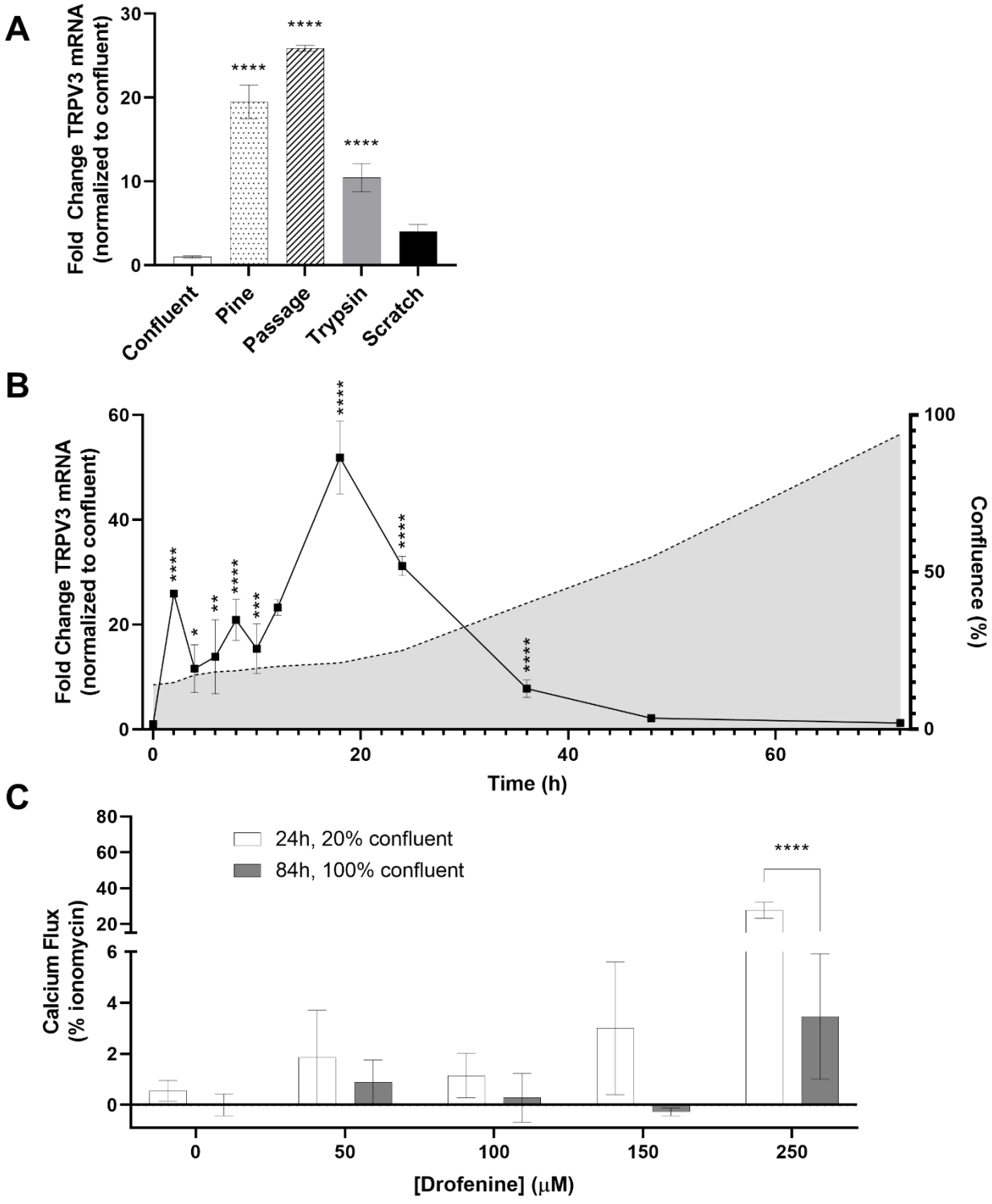

Downloaded from molpharm.aspetjournals.org at ASPET Journals on March 20, 2024

Molecular Pharmacology Fast Forward. Published on July 21, 2021 as DOI: 10.1124/molpharm.121.000280
This article has not been copyedited and formatted. The final version may differ from this version.

Figure 2

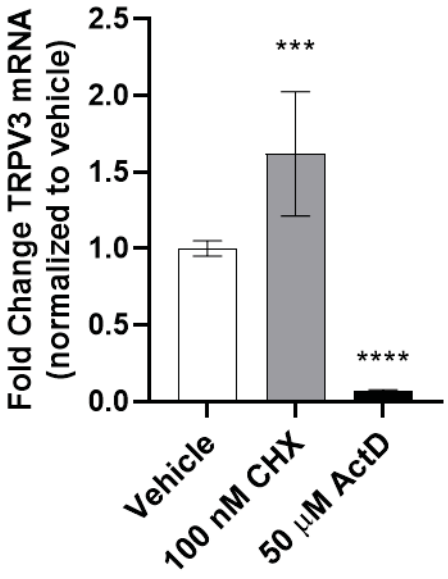

Downloaded from molpharm.aspetjournals.org at ASPET Journals on March 20, 2024

Molecular Pharmacology Fast Forward. Published on July 21, 2021 as DOI: 10.1124/molpharm.121.000280
This article has not been copyedited and formatted. The final version may differ from this version.

Figure 3

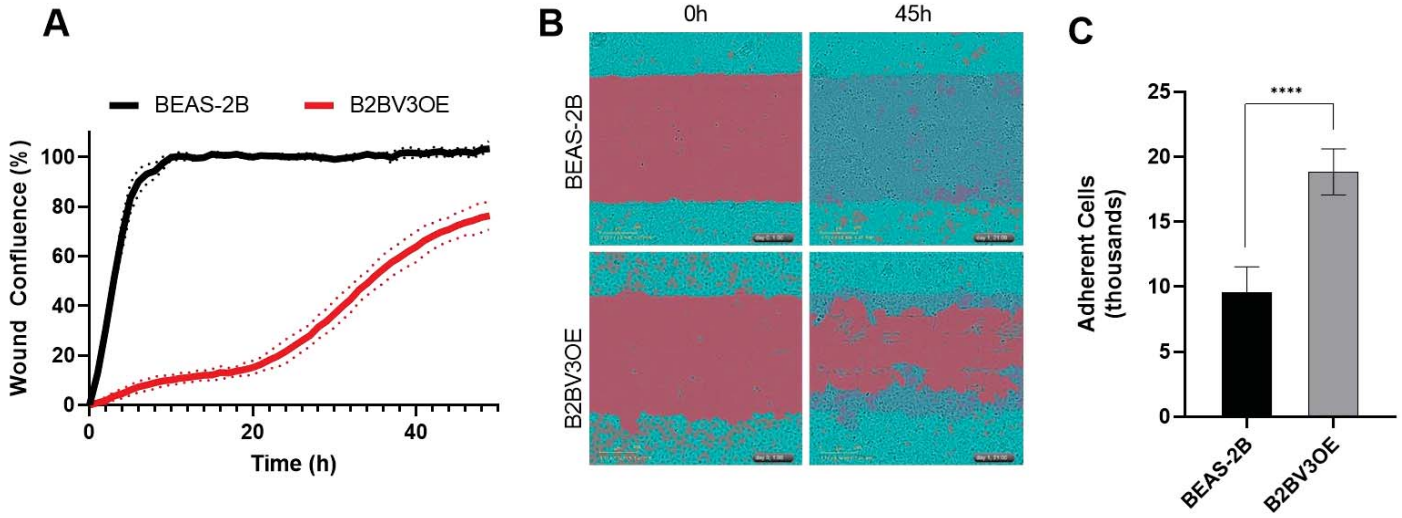

Downloaded from molpharm.aspetjournals.org at ASPET Journals on March 20, 2024

Molecular Pharmacology Fast Forward. Published on July 21, 2021 as DOI: 10.1124/molpharm.121.000280
This article has not been copyedited and formatted. The final version may differ from this version.

Figure 4

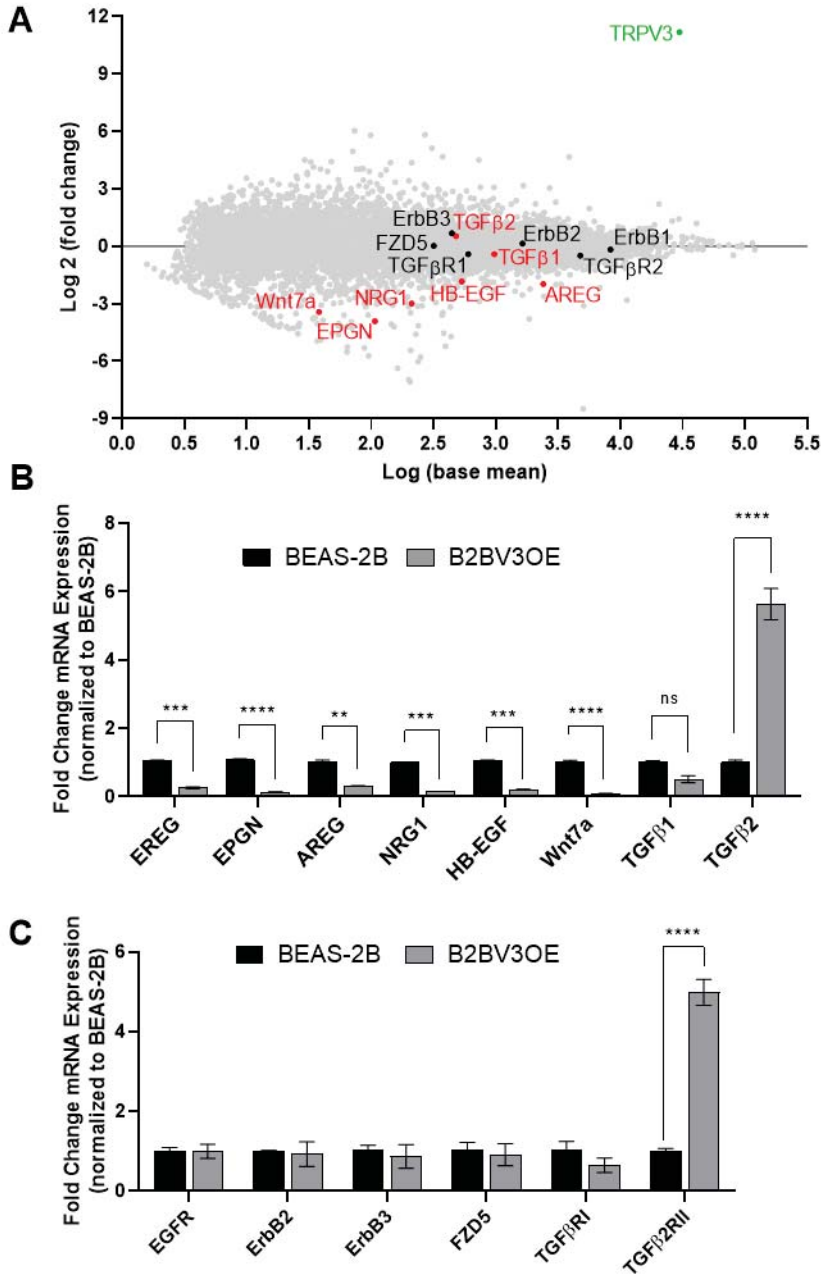

Downloaded from molpharm.aspetjournals.org at ASPET Journals on March 20, 2024

Molecular Pharmacology Fast Forward. Published on July 21, 2021 as DOI: 10.1124/molpharm.121.000280
This article has not been copyedited and formatted. The final version may differ from this version.

Figure 5

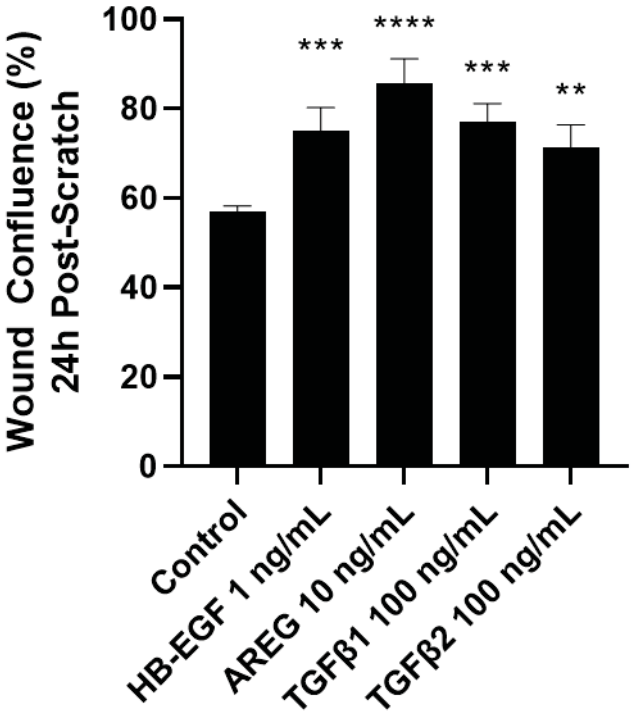

Downloaded from molpharm.aspetjournals.org at ASPET Journals on March 20, 2024

Molecular Pharmacology Fast Forward. Published on July 21, 2021 as DOI: 10.1124/molpharm.121.000280
This article has not been copyedited and formatted. The final version may differ from this version.

Figure 6

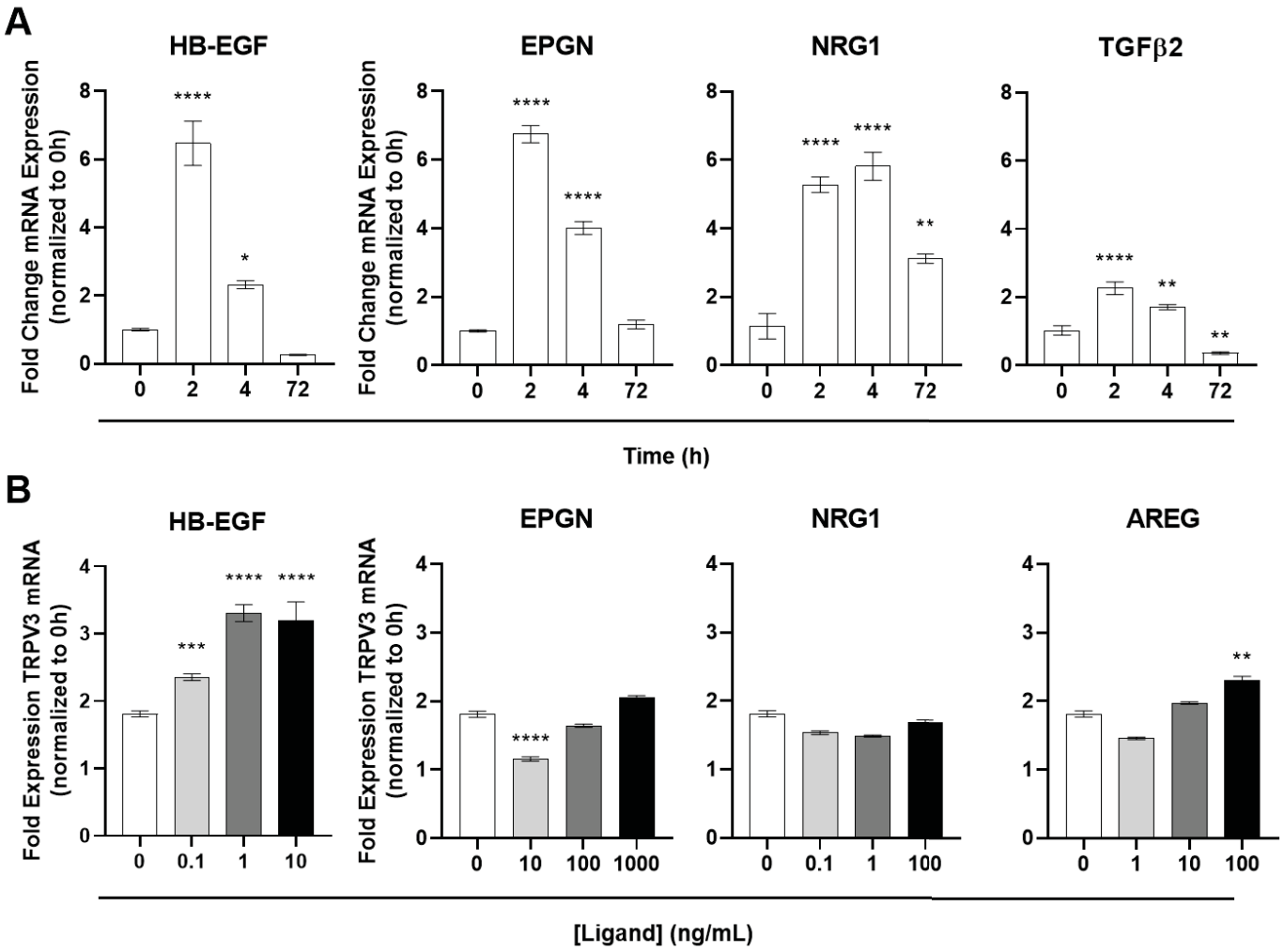

Downloaded from molpharm.aspetjournals.org at ASPET Journals on March 20, 2024

Molecular Pharmacology Fast Forward. Published on July 21, 2021 as DOI: 10.1124/molpharm.121.000280
This article has not been copyedited and formatted. The final version may differ from this version.

Figure 7

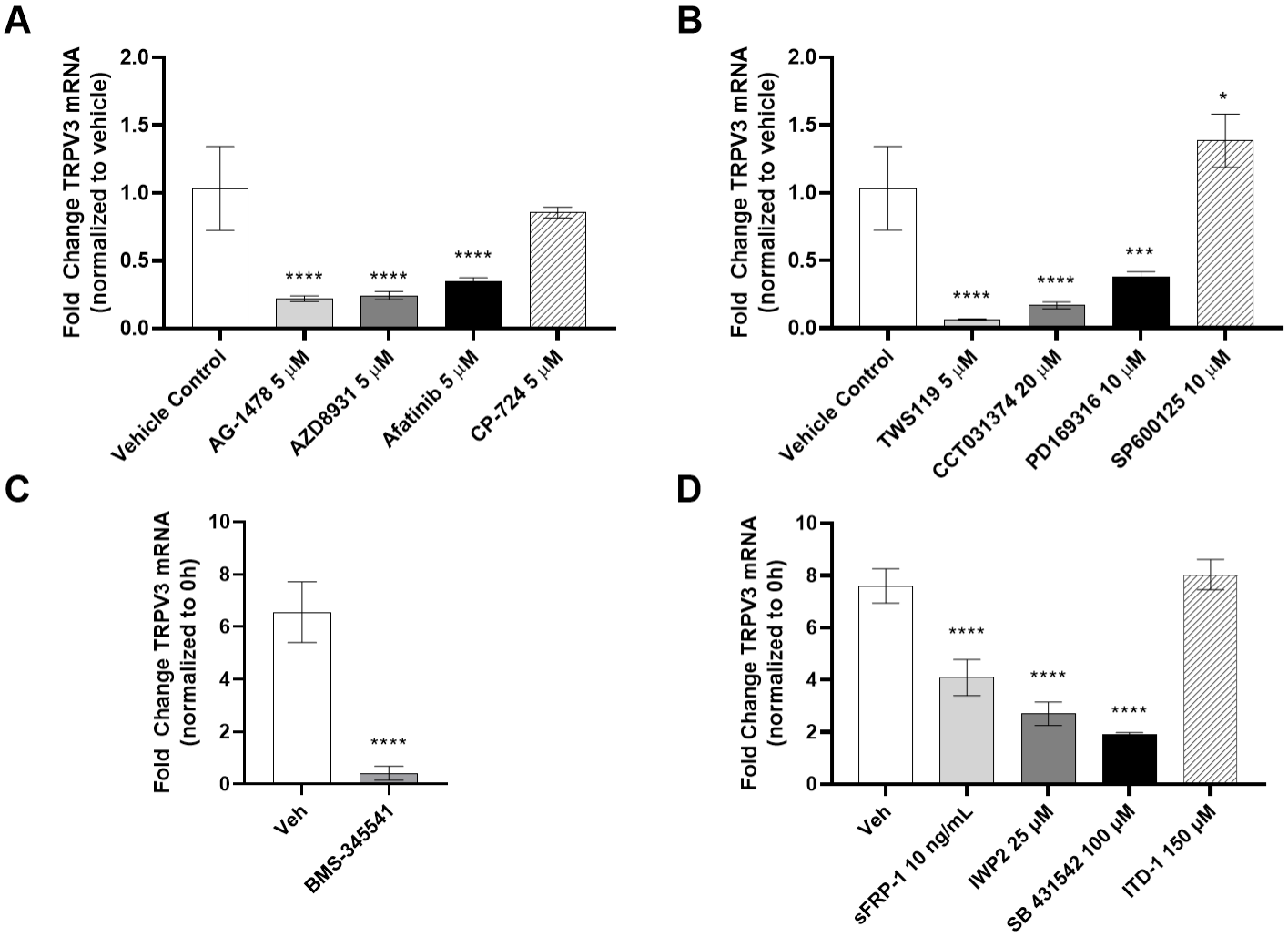

Downloaded from molpharm.aspetjournals.org at ASPET Journals on March 20, 2024

Molecular Pharmacology Fast Forward. Published on July 21, 2021 as DOI: 10.1124/molpharm.121.000280
This article has not been copyedited and formatted. The final version may differ from this version.

Figure 8

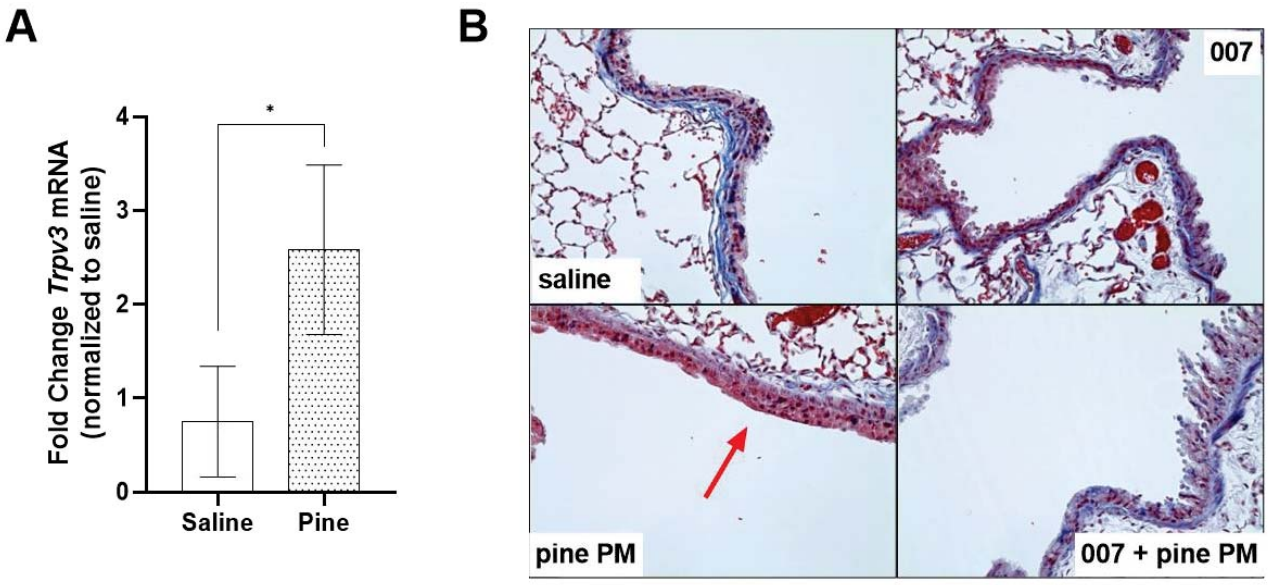

Downloaded from molpharm.aspetjournals.org at ASPET Journals on March 20, 2024

Molecular Pharmacology Fast Forward. Published on July 21, 2021 as DOI: 10.1124/molpharm.121.000280
This article has not been copyedited and formatted. The final version may differ from this version.

Figure 9

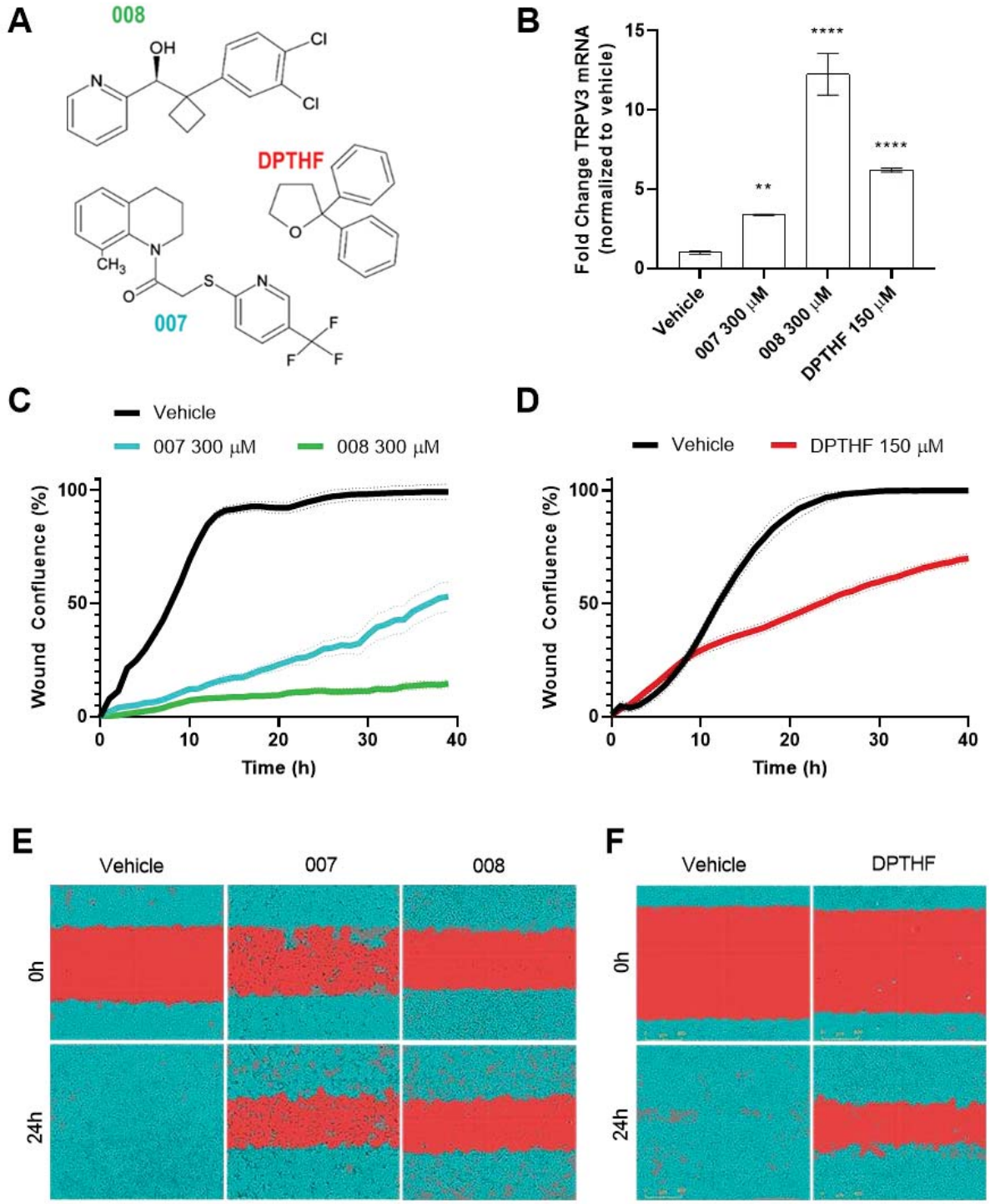

Downloaded from molpharm.aspetjournals.org at ASPET Journals on March 20, 2024

Molecular Pharmacology Fast Forward. Published on July 21, 2021 as DOI: 10.1124/molpharm.121.000280
This article has not been copyedited and formatted. The final version may differ from this version.

Figure 11

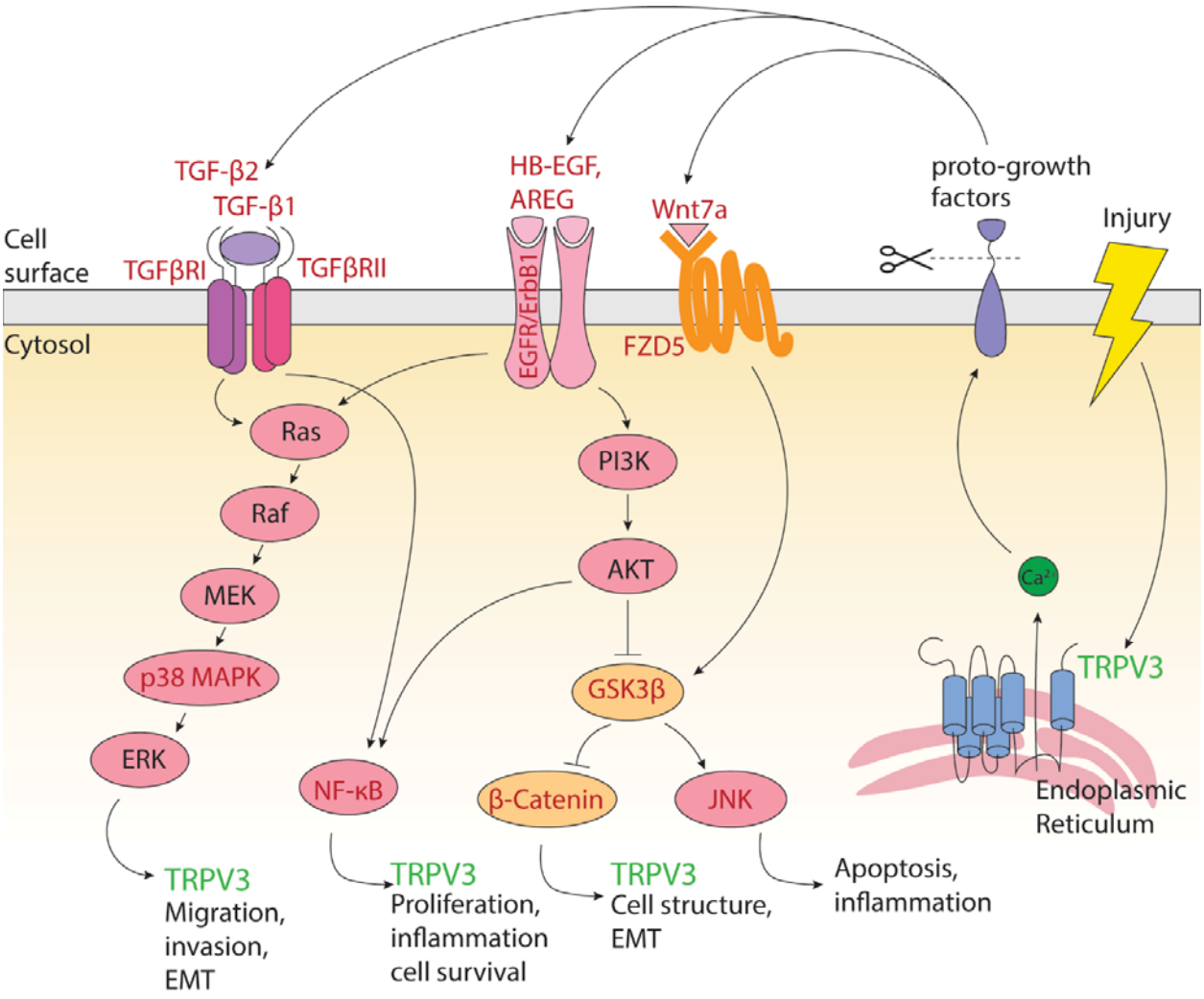

Downloaded from molpharm.aspetjournals.org at ASPET Journals on March 20, 2024

Supplementary Information:

Title: Dynamic Expression of TRPV3 and Integrated Signaling with Growth Factor Pathways During Lung Epithelial Wound Repair Following Wood Smoke Particle and Other Forms of Lung Cell Injury

Journal Title: Molecular Pharmacology

Authors: Katherine L. Burrell, Nam D. Nguyen, Cassandra E. Deering-Rice, Tosifa A. Memon, Marysol Almestica-Roberts, Emmanuel Rapp, Samantha N. Serna, John G. Lamb, and Christopher A. Reilly

Affiliations: (KLB, NDN, CEDR, TAM, MAR, ER, SNS, JGL, CAR) Department of Pharmacology and Toxicology, Center for Human Toxicology, University of Utah, 30 S 2000 E, Room 201 Skaggs Hall, Salt Lake City, Utah 84112, United States

Manuscript Number: MOLPHARM-AR-2021-000280

Methods:

Western blotting: HBEC3-KT cells were plated into T-25 flasks and harvested at various time points. BEAS2-B TRPV3OE cells were used as a positive control and harvested at 100% confluence. Cells were lysed using RIPA buffer (ThermoFisher) supplemented with 6M urea and fortified with Halt™ Phosphatase and Protease Inhibitor Cocktail (ThermoFisher). Total protein yields were determined the BCA protein assay (ThermoFisher) and 30 μg of protein/sample was loaded into 4-12% Bolt Bis-Tris 12-well gels (ThermoFisher). TRPV3 protein expression was measured using a 1:500 dilution of a mouse anti-TRPV3 primary antibody (75-043, NeuroMab, Davis CA), and band intensity was quantified using ImageJ software.

Immunocytochemistry: BEAS-2B and BEAS-2B TRPV3OE cells were plated on 8-well chamber slides, which were coated with LHC basal medium fortified with collagen (30 μg/mL), fibronectin (10 μg/mL), and bovine serum albumin fraction V (100 μg/mL). Cells were incubated for 2 hours to allow adhesion and then fixed with 4% paraformaldehyde and permeabilized with 0.2% Triton X-100. Blocking was done with 10% normal goat serum for 1h at room temperature (~22°C). To probe for TRPV3, cells were incubated with a mouse monoclonal primary antibody for TRPV3 (1:200; 73-043; Neuromab; Davis, CA) overnight at 4ºC, followed by incubation with a goat-anti-mouse secondary antibody conjugated with AlexaFluor594 (1:1000, A-11032, Invitrogen; Carlsbad, CA). After incubation with the antibodies, F-acting (phalloidin) was stained with ActinGreen conjugated with AlexaFluor488 (R37110, Invitrogen, Carlsbad, CA) and cell nuclei were stained with Hoechst 33342. Cells were then fixed with 4% paraformaldehyde and imaged.

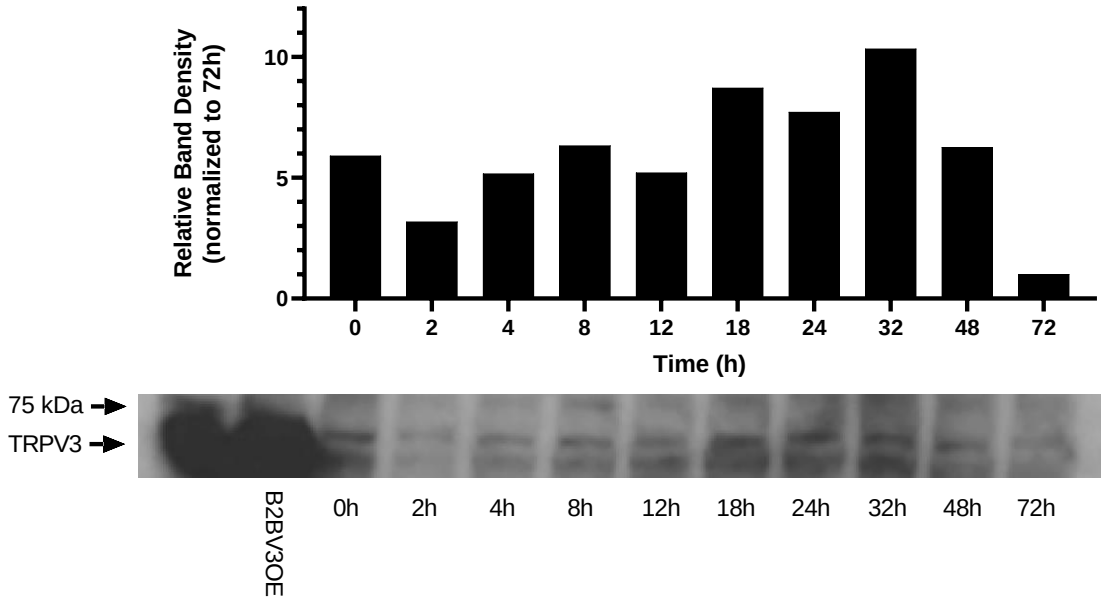

Supplemental Figure 1. Western blot analysis of TRPV3 protein (70 kDa) in HBEC3-KT cells versus time after cell passaging injury. Lysate from B2BV3OE cells was used as a positive control.

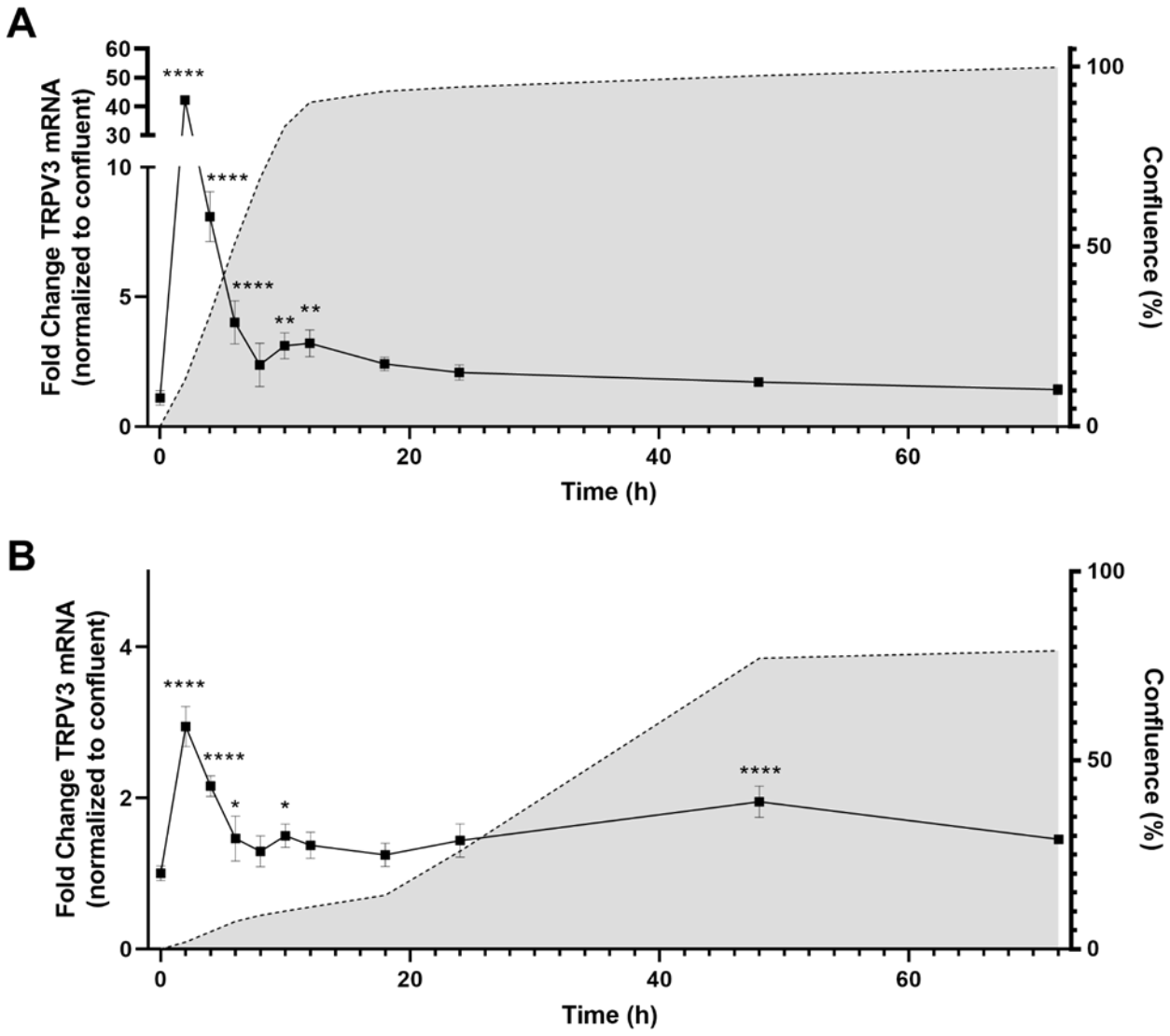

Supplemental Figure 2. TRPV3 expression over time in **A)** BEAS-2B and **B)** B2BV3OE cells. Data were normalized to 0h confluent control cells and are represented as the mean ± SD from *n* = 3 replicates. The grey fill (right y-axis) represents cell confluence. Statistical significance was determined using one-way ANOVA with the Dunnett post-test. **p* < 0.05, ***p* < 0.01, ****p* < 0.001, *****p* < 0.0001.

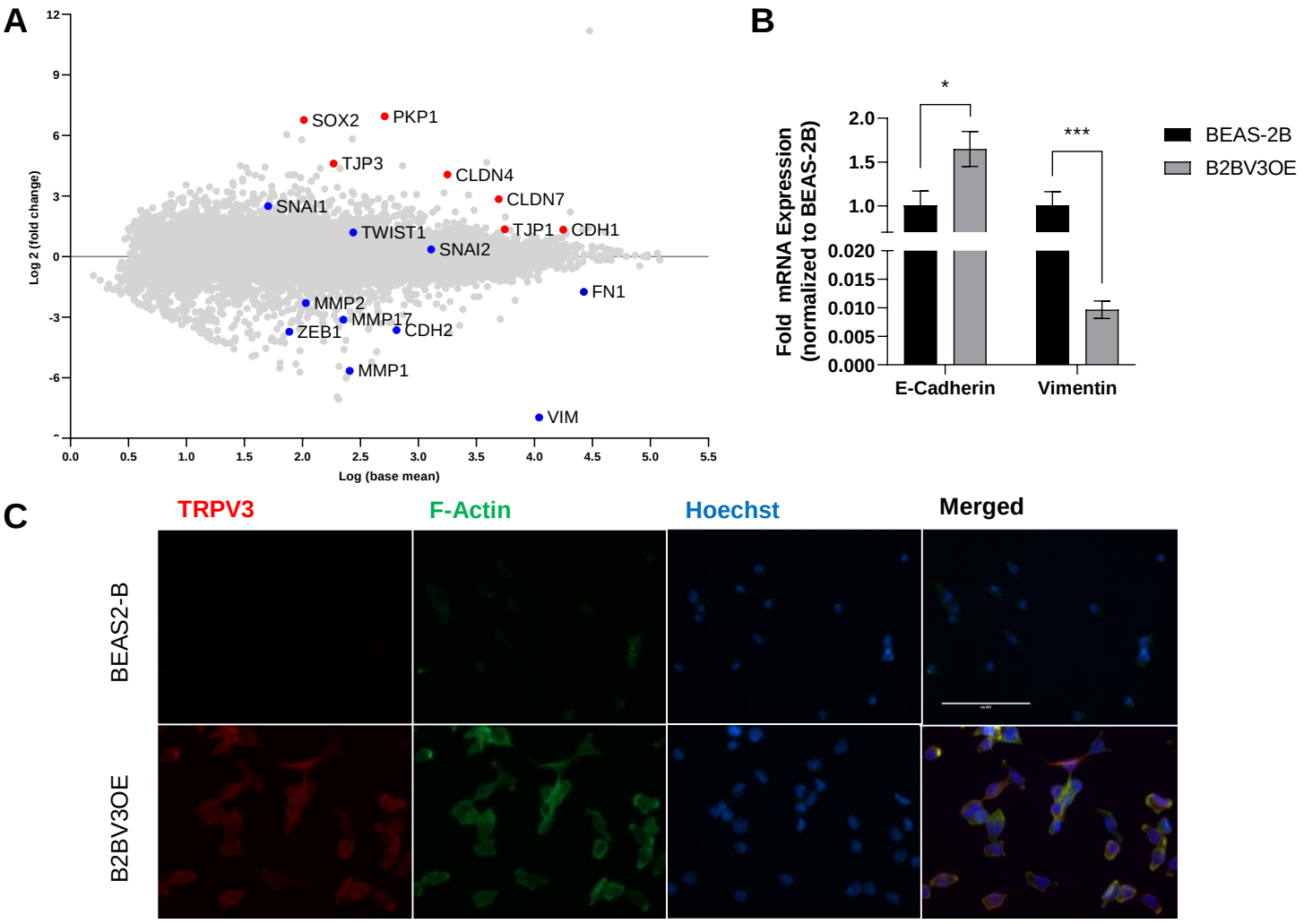

Supplemental Figure 3. Comparative expression of mRNA and protein for several epithelial and mesenchymal markers in BEAS2B and B2BV3OE cells. **A)** MA plot of RNAseq data illustrating differences in epithelial (red) and mesenchymal (blue) markers. **B)** Quantitative PCR results comparing vimentin and E-cadherin mRNA expression. **C)** Immunocytochemical analysis of TRPV3 (red) and F-Actin (green) in BEAS-2B and B2BV3OE cells.

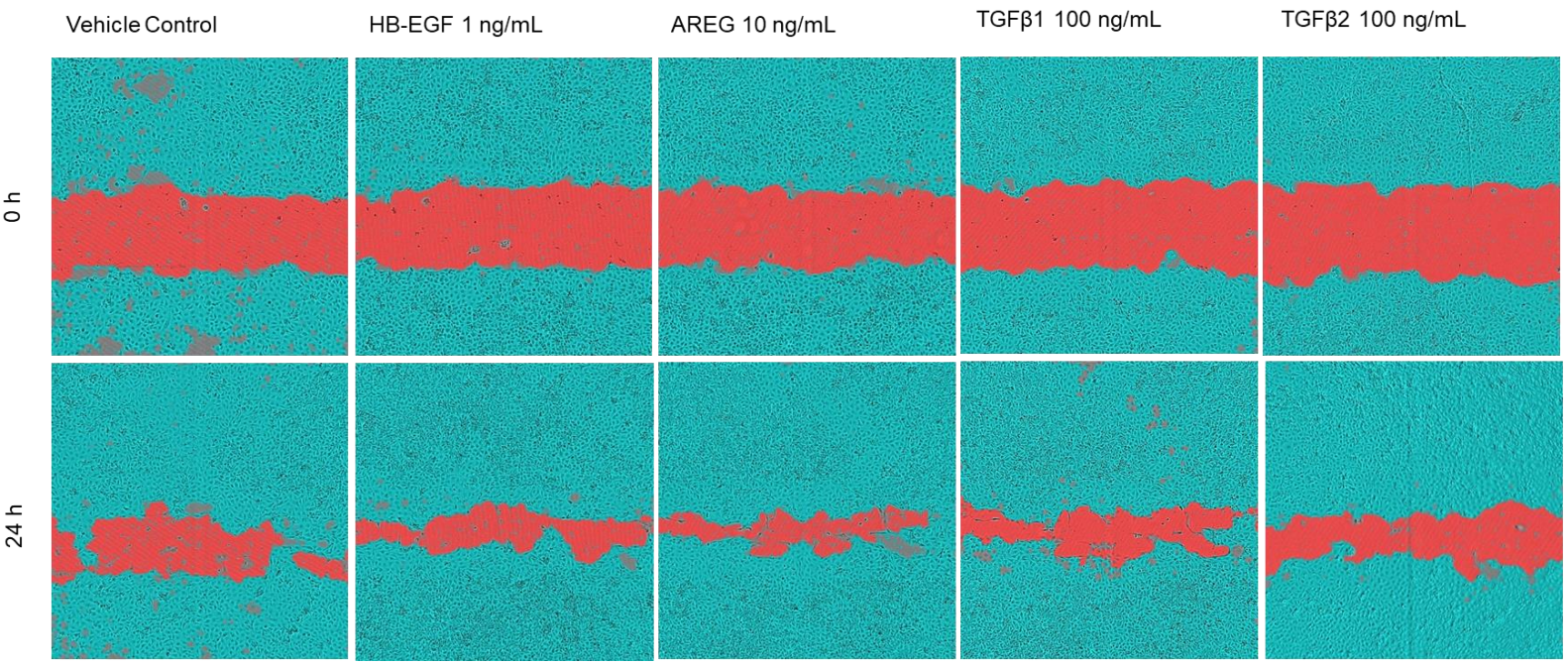

Supplemental Figure 4. Scratch wound repair images of B2BV3OE cells at 0 and 24h after injury when cultured in conditioned media with or without 1 ng/mL recombinant HB-EGF, 10 ng/mL AREG, 100 ng/mL TGFβ1 or 100 ng/mL TGFβ2.

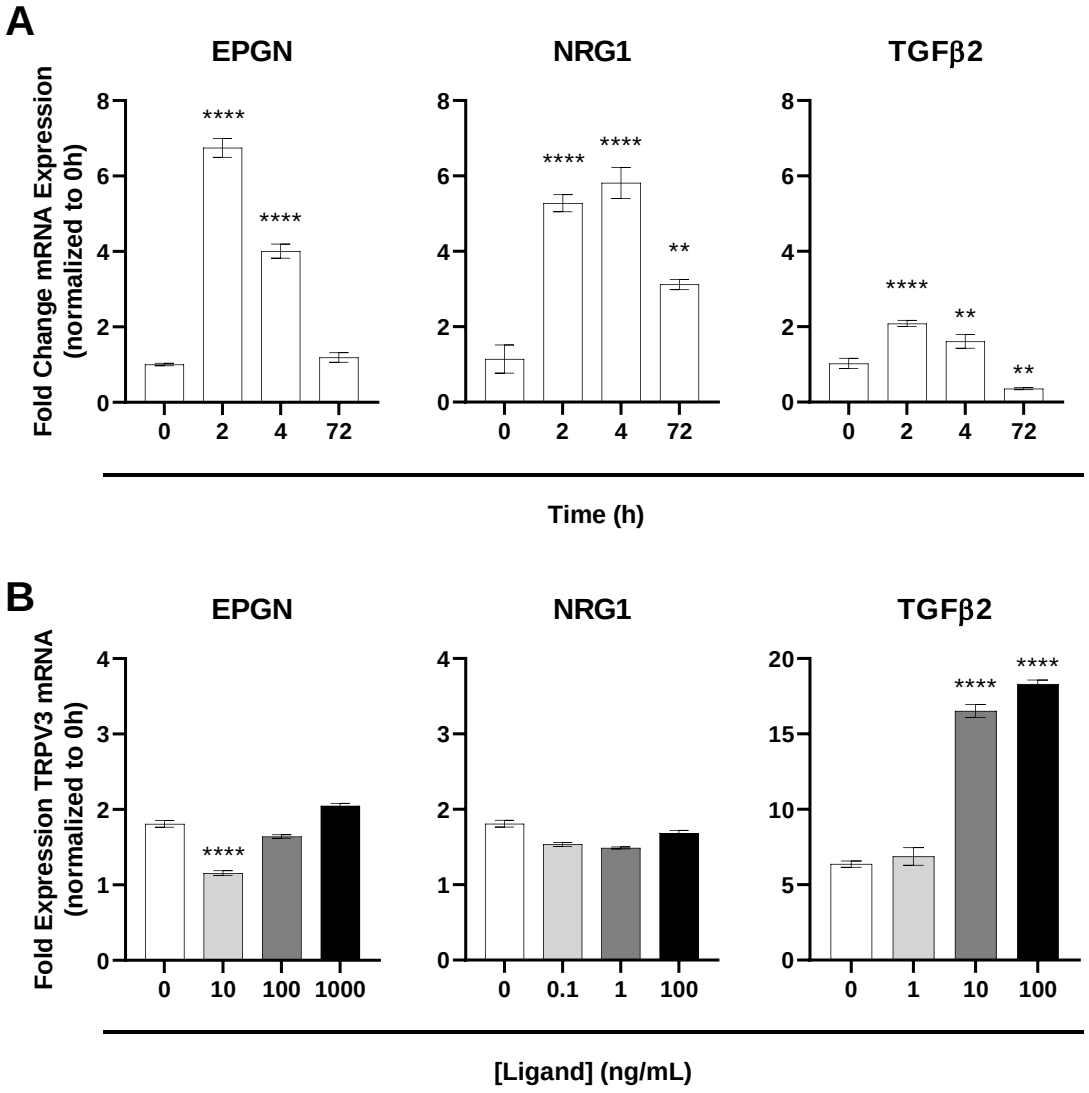

Supplemental Figure 5. A) Time-dependent induction of EPGN, NRG1 and TGFβ2 mRNA in HBEC3-KT cells compared to 0h confluent cells. **B)** TRPV3 mRNA induction 2h post-passaging injury with EPGN, NRG1 and TGFβ2 growth factor supplementation to conditioned media. Data were normalized to 0h, non-injured cells and presented as mean ± SD from $n \geq 3$ replicates. Significance was determined using one-way ANOVA with the Dunnett post-test. *$p < 0.05$, **$p < 0.01$, ***$p < 0.001$, ****$p < 0.0001$.

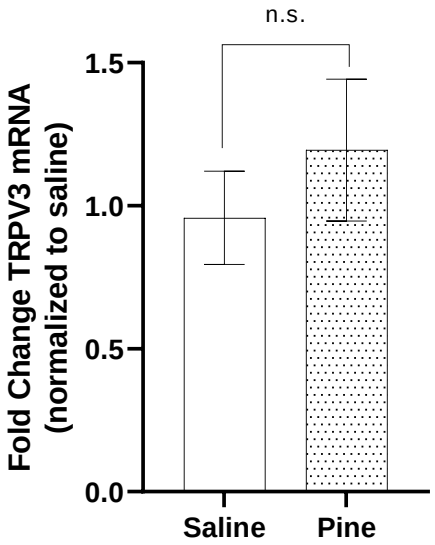

Supplemental Figure 6. *Trpv3* mRNA expression in distal airway/parenchymal tissue isolated from C57/BL6 mice treated sub-acutely with saline or 0.5 mg/kg pine PM via OPA. Data represent the mean ± SD from $n \geq 3$ for each treatment and significance was determined using an unpaired t-test setting $p < 0.05$ as the level for significance.

	Uninjured/100% Confluent (0h, Normalized)	Cell Passaging	Trypsin	Mechanical/Scratch Wound	Pine PM
HBEC3-KT	1.0 ± 0.1	**25.9 ± 0.3**	**11 ± 1**	*4.0 ± 0.7*	**20 ± 2**
BEAS-2B	1.1 ± 0.2	**42.3 ± 0.9**	1.9 ± 0.6	**6.3 ± 0.6**	**16 ± 1**
B2BV3OE	1.00 ± 0.08	3.0 ± 0.2	----	----	----
Lobar Bronchial	1.00 ± 0.03	*3.89 ± 0.06*	----	----	**6 ± 1**

Supplemental Table 1. Induction of TRPV3 mRNA in multiple human airway epithelial cell lines 2h after various types of *in vitro* injury. Data represent the mean ± SD from $n \geq 3$ for each injury model and are normalized to the confluent control of each cell line. Statistical significance was determined using two-way ANOVA with the Tukey post-test. $p < 0.05$ (values in *italics*), ****$p < 0.0001$ (values in **bold**).

Movie S1 (separate file). Videos showing the mechanical/scratch wound repair process for BEAS-2B (left) and B2BV3OE (right) cells over a period of 36h.

Movie S2 (separate file). Videos comparing the mechanical/scratch wound repair process for HBEC3-KT cells treated with media (vehicle, left) and the TRPV3 antagonists 007(300 μM, middle) or 008 (300 μM, right).

Movie S3 (separate file). Videos showing the mechanical/scratch wound repair process for HBEC3-KT cells treated with media (vehicle, left) and the TRPV3 antagonists DPTHF (150 μM, right).